AFRL-AFOSR-UK-TR-2016-0016

The physics of ultrabroadband frequency comb generation and optimized combs for measurements in fundamental physics

John Dudley
UNIVERSITE DE BESANCON

07/02/2016
Final Report

DISTRIBUTION A: Distribution approved for public release.

Air Force Research Laboratory
AF Office Of Scientific Research (AFOSR)/ IOE
Arlington, Virginia 22203
Air Force Materiel Command

REPORT DOCUMENTATION PAGE

Form Approved
OMB No. 0704-0188

The public reporting burden for this collection of information is estimated to average 1 hour per response, including the time for reviewing instructions, searching existing data sources, gathering and maintaining the data needed, and completing and reviewing the collection of information. Send comments regarding this burden estimate or any other aspect of this collection of information, including suggestions for reducing the burden, to Department of Defense, Executive Services, Directorate (0704-0188). Respondents should be aware that notwithstanding any other provision of law, no person shall be subject to any penalty for failing to comply with a collection of information if it does not display a currently valid OMB control number.
PLEASE DO NOT RETURN YOUR FORM TO THE ABOVE ORGANIZATION.

1. REPORT DATE *(DD-MM-YYYY)*	2. REPORT TYPE	3. DATES COVERED *(From - To)*
02-07-2016	Final	01 Feb 2013 to 31 Jan 2016

4. TITLE AND SUBTITLE
The physics of ultrabroadband frequency comb generation and optimized combs for measurements in fundamental physics

5a. CONTRACT NUMBER

5b. GRANT NUMBER
FA8655-13-1-2137

5c. PROGRAM ELEMENT NUMBER
61102F

6. AUTHOR(S)
John Dudley

5d. PROJECT NUMBER

5e. TASK NUMBER

5f. WORK UNIT NUMBER

7. PERFORMING ORGANIZATION NAME(S) AND ADDRESS(ES)
UNIVERSITE DE BESANCON
1, RUE CLAUDE GOUDIMEL
BESANCON, 25000 FR

8. PERFORMING ORGANIZATION REPORT NUMBER

9. SPONSORING/MONITORING AGENCY NAME(S) AND ADDRESS(ES)
EOARD
Unit 4515
APO AE 09421-4515

10. SPONSOR/MONITOR'S ACRONYM(S)
AFRL/AFOSR IOE

11. SPONSOR/MONITOR'S REPORT NUMBER(S)
AFRL-AFOSR-UK-TR-2016-0016

12. DISTRIBUTION/AVAILABILITY STATEMENT
A DISTRIBUTION UNLIMITED: PB Public Release

13. SUPPLEMENTARY NOTES

14. ABSTRACT
Work finished and report in.

15. SUBJECT TERMS
phase dynamics of optical frequency combs, equivalent higher-order susceptibility, higher-order phase-matched cascaded frequency gene, high harmonic generation, fine structure constant measurements, -envelope phase stabilization, ultra fast laser modeling, EOARD

16. SECURITY CLASSIFICATION OF:			17. LIMITATION OF ABSTRACT	18. NUMBER OF PAGES	19a. NAME OF RESPONSIBLE PERSON
a. REPORT	b. ABSTRACT	c. THIS PAGE			GONGLEWSKI, JOHN
Unclassified	Unclassified	Unclassified	SAR	48	**19b. TELEPHONE NUMBER** *(Include area code)* 011-44-1895-616007

Standard Form 298 (Rev. 8/98)
Prescribed by ANSI Std. Z39.18

FINAL REPORT

Grant No. 12RSW137

The physics of ultrabroadband frequency comb generation and optimized combs for measurements in fundamental physics

Grantee: John Dudley

CNRS Institut FEMTO-ST

Université de Franche-Comté

Besançon, France

Project Grant Period : 2/1/2013 – 31/1/2016

Table of Contents

DISTRIBUTION A. Approved for public release: distribution unlimited.

1. Summary of Activities Carried Out

This project had as its aim to carry out targeted numerical and experimental studies into the properties of optical frequency comb sources. The generation of frequency combs is intimately connected with the nonlinear spectral broadening that occurs in optical fibers due to the Kerr effect, and our initial work focussed on fundamental studies examining the sensitivity of such nonlinear spectral broadening to input noise, and the development of techniques to reduce such noise with the presence of an external seed source. To perform fundamental studies of this process, we considered the case of "spontaneous" four wave mixing or modulation instability, which is the noise-driven analogue of the process generating frequency combs. Our experimental set-up is shown below and illustrates how the nonlinear spectral broadening induced by the 20 MHz pump laser source in 9.5 m of highly nonlinear fiber (HNLF) was combined with a "seeding" source whose aim was to lower the threshold for spectral broadening by stimulating it from either a narrowband (100 kHz linewidth) continuous wave or a (partially) coherent seed.

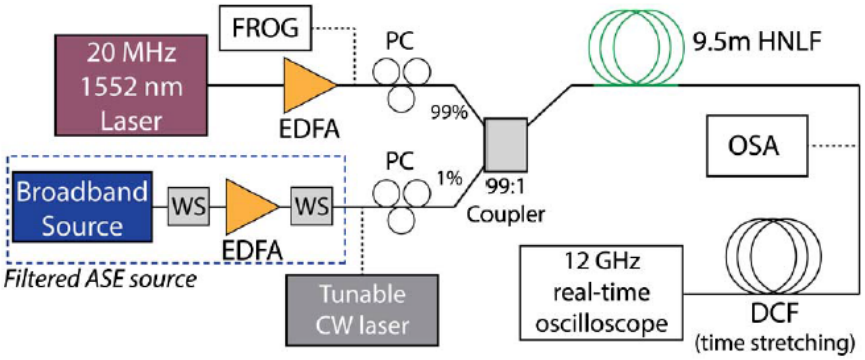

Figure 1: Experimental Setup used

Our experiments showed control of both the spectral and noise properties of optical fibre spectral broadening using an incoherent seed with power at the 10^{-6} level relative to the pump, and varying the seed wavelength revealed enhancement of the spectrally-broadened bandwidth and improvement in signal-to-noise ratio as the seed coincides with the peak of the calculated four wave mixing (modulation instability) gain. Stochastic nonlinear Schrödinger equation simulations were shown to be in very good agreement with experiment. This work was reported in Opt. Lett. **38** 5338 (2013) and in a number of conferences (see list below).

An important feature of our work was the development of a real time technique suitable for the measurement of spectral fluctuations, and the grant was indispensable in allowing us to purchase and optimise the necessary equipment. This real-time technique has become a standard technique allowing the study of nonlinear spectral broadening under a wide range of conditions. Our work performed using this technique was also reported in a summary paper which was selected as a highlight of Optics in 2013 by the Optical Society of America in Optics and Photonics News, Dec (2013).

The results of this project have direct impact on the understanding of the nonlinear wave mixing interactions in frequency combs, and will feed into future studies of comb dynamics and dissipative soliton characterisation using real-time measurement techniques.

DISTRIBUTION A. Approved for public release: distribution unlimited.

Publications

Key publications specifically linked to the studies funded by the grant are:

D. M. Nguyen, T. Godin, S. Toenger, Y. Combes, B. Wetzel, T. Sylvestre, et al., "Incoherent resonant seeding of modulation instability in optical fiber," Optics Letters, **38**, 5338-5341, (2013)

T. Godin, B. Wetzel, J. M. Dudley, G. Herink, F. Dias, G. Genty, B. Jalali, C. Ropers, D.R. Solli "Ultrafast Single-Shot Measurements in Modulation Instability and Supercontinuum," Optics and Photonics News, **24**(12) pp. 55-55 (2013) special issue on Optics in 2013

The results obtained in this work have been presented at a number of Keynote and Plenary conference presentations given by the Principal Investigator in 2013-2015

J. M. Dudley, "The Key Enabling Technologies of Photonics," Plenary Lecture at IEEE/ASME International Conference on Advanced Intelligent Mechatronics, July 8-11, Besançon, France (2014)

J. M. Dudley, "Extreme Processes in Nonlinear Fiber Optics," The Rank Prize Funds Symposium on New Horizons in Nonlinear Fibre Optics June 16-19, Grasmere, UK (2014)

J. M. Dudley, "Frontiers of Nonlinear Optics," 18th meeting of the Czech-Slovak Physical Societies, Olomouc, Czech republic, Sept 16-19 (2014)

J. M. Dudley, "Unexpected Ultrafast – New Frontiers in the Physics and. Applications of Ultrafast Optics," ICMAT 2015, 28 June – 3 July, Singapore (2015)

DISTRIBUTION A. Approved for public release: distribution unlimited.

Annexes

The annexes contain reprints of the key publications listed above, together with the slides of a Keynote talk delivered at the Photonics Global Conference held in Singapore in 2015.

DISTRIBUTION A. Approved for public release: distribution unlimited.

Incoherent resonant seeding of modulation instability in optical fiber

Duc Minh Nguyen,[1] Thomas Godin,[1] Shanti Toenger,[1] Yves Combes,[1] Benjamin Wetzel,[1] Thibaut Sylvestre,[1] Jean-Marc Merolla,[1] Laurent Larger,[1] Goëry Genty,[2] Frédéric Dias,[3] and John M. Dudley[1,*]

[1]*Institut FEMTO-ST, UMR 6174 CNRS-Université de Franche-Comté, Besançon, France*

[2]*Department of Physics, Tampere University of Technology, Tampere, Finland*

[3]*School of Mathematical Sciences, University College Dublin, Belfield, Dublin 4, Ireland*

**Corresponding author: john.dudley@univ-fcomte.fr*

Received September 18, 2013; revised November 7, 2013; accepted November 7, 2013; posted November 8, 2013 (Doc. ID 197950); published December 9, 2013

We report control of the spectral and noise properties of spontaneous modulation instability (MI) in optical fiber using an incoherent seed with power at the 10^{-6} level relative to the pump. We sweep the seed wavelength across the MI gain band, and observe significant enhancement of MI bandwidth and improvement in the signal-to-noise ratio as the seed coincides with the MI gain peak. We also vary the seed bandwidth and find a reduced effect on the MI spectrum as the seed coherence decreases. Stochastic nonlinear Schrödinger equation simulations of spectral and noise properties are in excellent agreement with experiment. © 2013 Optical Society of America

OCIS codes: (030.1640) Coherence; (190.4370) Nonlinear optics, fibers; (190.4380) Nonlinear optics, four-wave mixing; (320.7140) Ultrafast processes in fibers.

http://dx.doi.org/10.1364/OL.38.005338

Modulation instability (MI) in the anomalous dispersion regime of an optical fiber is associated with the exponential growth of low amplitude noise on an incident continuous-wave (CW) or quasi-CW pump. The instability leads to strong temporal modulation of the pump and the growth of distinct sidebands in the spectrum [1–3]. MI is one of the fundamental nonlinear processes in many fields such as optics, plasma physics, and hydrodynamics, and it has become the subject of significant recent interest because of links with the emergence of giant "rogue wave" instabilities on the ocean [4,5]. Noise-driven MI is also a key mechanism in fiber supercontinuum (SC) generation using long pulses, and has been extensively studied in the context of high-power broadband source development [6].

The spectral structure and noise properties of MI-driven SC generation have been previously shown to be highly sensitive to the presence of a weak copropagating seed, and numerical studies have been confirmed experimentally for both femtosecond and picosecond pulse pumping [7–11]. The fact that a low amplitude seed can strongly affect MI can be understood physically because the seed creates an initial modulation on the pump that will see preferential growth relative to any broadband noise. However, all previous studies in this field have been carried out with strongly coherent seed and pump sources using either a low amplitude pulse replica derived from the pump [10] or a narrow linewidth CW laser [11].

In this Letter, we show that the strong influence of an external seed on MI dynamics is still observed even when the external seed is only partially coherent. Specifically, using broadband amplified spontaneous emission (ASE) to seed picosecond MI, we observe resonant enhancement of the MI spectral width and noise reduction as we sweep the seed wavelength across the peak of the MI gain curve. We also study the influence of the ASE seed bandwidth on the observed dynamics, and show that the effect of the seed is reduced when its associated coherence time decreases below the duration of the temporal pump pulses. This clearly highlights the importance of a stable amplitude modulation in effectively seeding MI dynamics. Our results are shown to be in excellent agreement with generalized stochastic nonlinear Schrödinger equation (GNLSE) simulations. Note that this work is in contrast to previous studies of spontaneous MI in the spatial domain that use a strong incoherent pump and coherent seeds [12–14]. Here, we study the regime in which the spontaneous MI initiated from a coherent pump in the time domain is modified by a very weak incoherent seed.

Figure 1 shows the experimental setup. Input pulses at 1552 nm and 20 MHz repetition rate are generated from a picosecond fiber laser (Pritel FFL-500) before amplification in an erbium-doped fiber amplifier (EDFA). The pump pulses after the EDFA are characterized using an optical spectrum analyzer (OSA, Anritsu MS9710B) and frequency-resolved optical gating (FROG).

The pump pulses have 3.8 ps temporal width (FWHM) and a spectrum with characteristic features of self-phase modulation. The time–bandwidth product is $\Delta\tau\Delta\nu \sim 0.42$. The seed was derived from an amplified ASE source (Highwave HWT-BS-B1-2) spectrally shaped with two tunable filters (Finisar Waveshaper 4000S) before and after the amplifier to ensure precise control over spectral bandwidth and power.

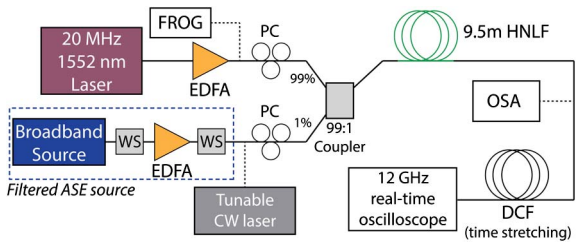

Fig. 1. Experimental setup. DCF, dispersion compensating fiber; PC, polarization controller; WS, waveshaper.

 © 2013 Optical Society of America

DISTRIBUTION A. Approved for public release: distribution unlimited.

The seed could be configured to have variable bandwidth from 1 to 36 nm with central wavelength tunable over 1527–1550 nm. The pump pulses were combined with the seed and injected into 9.5 m of Ge-doped highly nonlinear fiber (OFS HNLF). At the HNLF input, the average pump power was 6.4 mW ($P_0 = 68$ W peak power), and the average ASE seed power was 90 μW, i.e., 10^6 times lower than the pump.

The average spectra at the HNLF output were recorded using the OSA and studied as a function of ASE central wavelength and bandwidth. OSA measurements were complemented using dispersive time stretching that allows the shot-to-shot spectral fluctuations to be directly measured [15–17]. This technique is based on the fact that the intensity of a temporal field evolves into its Fourier transform with sufficient propagation in a linear dispersive medium of length L. For total dispersion $\beta_{2S}L$, an input pulse $U(t)$ with Fourier transform $\tilde{U}(\omega)$ spreads temporally to have intensity that is a scaled replica of the input spectrum $|U_z(t)|^2 \propto |\tilde{U}(t/(2\beta_{2s}L))|^2$. With our setup, dispersive time stretching was implemented using $L = 875$ m of dispersion compensating fiber (DCF) with $\beta_{2S}L = +130$ ps^2 such that the ~ns stretched pulses could be easily detected in real time using a 20 GHz detector (New Focus Model 1414) and 12 GHz oscilloscope (Tektronix TDS 6124C). The equivalent spectral resolution with this setup was 0.8 nm.

We first present numerical simulations to illustrate the expected influence of the low amplitude seed on the MI structure for our parameters. We use the GNLSE previously shown to model the statistics of SC generation including dispersion to arbitrary order, self-steepening, and Raman scattering [18]. For the purposes of defining notation, we write this to third-order dispersion here in the form $A_z + i\beta_2/2A_{tt} - \beta_3/6A_{ttt} - i\gamma|A|^2A = 0$, where $A(z,t)$ is the pulse envelope, nonlinear coefficient $\gamma = 10.5$ W^{-1} km^{-1}, and dispersion parameters $\beta_2 = -5.24$ ps^2 km^{-1} and $\beta_3 = 4.29 \times 10^{-2}$ ps^3 km^{-1}. Note that Raman scattering and self-steepening were found to have negligible influence on the results. We used for the pump pulse the parameters as measured by the FROG system. For the ASE seed, we used a Gaussian fit to the filtered spectrum with random phase and amplitude normalization to experimental average power.

Figure 2 shows numerical results for a fixed seed wavelength of 1531 nm near the maximum of the MI gain curve. Simulations are performed with different initial random noises to determine both average MI spectra and noise statistics.

We plot 500 individual realizations from the simulation ensemble as well as their mean. The CW seed was numerical resolution-limited. We also plot the spectral coherence and the coefficient of variation C_v defined for a distribution as $C_v = \sigma/\mu$ where σ and μ are the standard deviation and mean at a specific wavelength, respectively, such that C_v yields a measure of noise to signal [8,15].

Figure 2(a) with no seed shows a bandwidth of 100 nm at the −50 dB level. When MI is seeded by a CW seed we see a significant increase in the bandwidth and reduction in the shot-to-shot spectral fluctuations [see Fig. 2(b)]. The improved coherence across the MI bandwidth in this

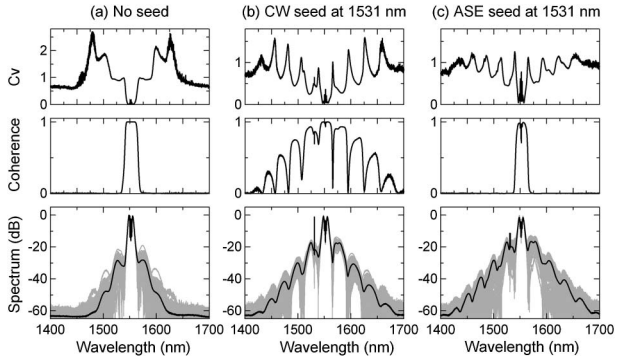

Fig. 2. Simulation results: MI spectra for (a) no seed, (b) CW seed, (c) 1 nm bandwidth ASE seed. Individual realizations are shown in gray, average in black. Upper panels show second-order spectral coherence and C_v.

case is expected because MI develops from low amplitude coherent modulation due to beating between the pump and the seed [7]. Significantly, our results in Fig. 2(c) show how this effect is also observed using a finite bandwidth ASE seed with an increase in bandwidth comparable to the case of a CW seed. However, the partially coherent nature of the ASE does not yield comparable coherence improvement across the bandwidth. Nevertheless, comparison of C_v in both cases shows that a partially coherent seed still provides a stabilization of spectral shot-to-shot fluctuations similar to that seen in the CW seed case. These simulation results reveal a key novelty in predicting that even partially coherent ASE at very low amplitude can have a drastic impact on MI dynamics as confirmed by our experiments below.

Our first experiments examined how the MI spectral structure and noise properties vary as a function of ASE seed wavelength for a fixed 1 nm ASE bandwidth. The MI gain band extends from zero detuning up to a maximum frequency of $(1/2\pi)\ (4\gamma P_0/|\beta_2|)^{1/2} = 3.72$ THz. Peak MI gain is at 2.63 THz. With our setup, we were able to explore a detuning range from 0 to 3.2 THz (i.e., 1527–1552 nm) that includes the MI gain peak. Due to the limitations of the filters, we inject the seed with positive frequency detuning (i.e., on the short wavelength side of the pump), but simulations show that the same effect is observed irrespective of the detuning sign.

Figure 3(a) shows a false-color plot of the measured spectrum when scanning the seed across the MI gain curve. As the seed wavelength is varied, we see a dramatic effect on the MI spectral structure, with the amount of seed-induced spectral broadening following closely the calculated MI gain curve.

When the seed is close to the pump or in the region of low MI gain, there is little spectral modification, but as the seed frequency approaches the peak of MI gain we see a significant effect, with the generation of multiple MI sidebands. This is in excellent agreement with numerical simulations shown in Fig. 3(a) for an ensemble of 500 numerical realizations from which the mean spectrum was calculated. The remarkable visual correspondence with the experimental results confirms the ability of the stochastic NLSE simulations to reproduce the experimentally observed spectral structure at all seed

DISTRIBUTION A. Approved for public release: distribution unlimited.

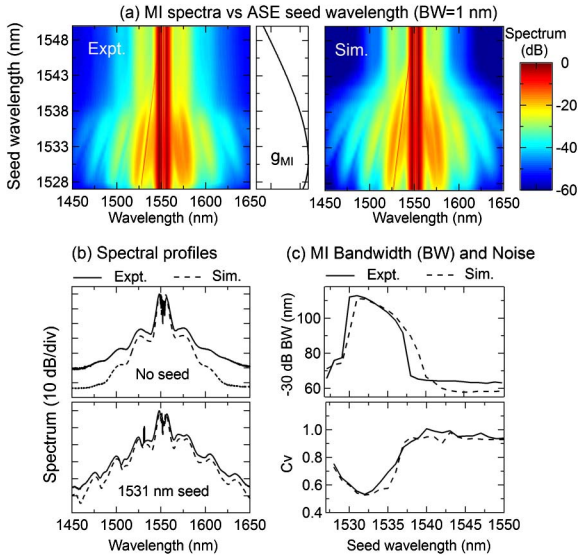

Fig. 3. (a) MI spectral profiles as ASE seed wavelength is varied. The MI gain curve is shown on the center. (b) Experimental average spectra (solid) and numerical results (dashed) for unseeded (top) and for a 1531 nm seed (bottom). (c) Seed wavelength dependence of –30 dB MI bandwidth (top) and C_v at 1580 nm (bottom).

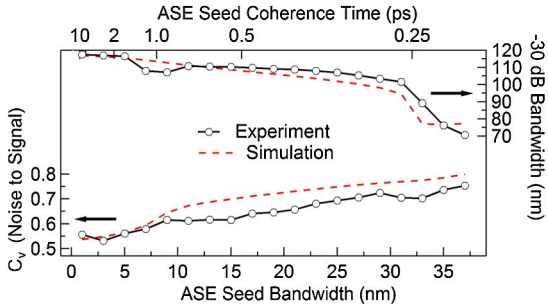

Fig. 4. Experimental results showing the variation with ASE seed bandwidth of (top) –30 dB MI bandwidth and (bottom) C_v at the seed central wavelength.

wavelengths. To compare experiments and simulations explicitly, Fig. 3(b) shows the experimental average spectra with the corresponding numerical results both for the unseeded case and near the MI gain peak with a 1531 nm seed.

To illustrate more clearly the increase in the spectral bandwidth, Fig. 3(c) shows the spectral expansion at the –30 dB level as a function of seed wavelength, once again in very good agreement with the numerical simulations. We also characterized the intensity noise at 1580 nm using real-time dispersive time stretching as described above. From the measured time series, it is straightforward to compute the coefficient of variation C_v, which is plotted as a function of ASE seed wavelength in Fig. 3(c). Again experimental results are compared with stochastic numerical simulations, and both show clear noise reduction as the seed wavelength approaches the frequency of maximum MI gain.

This particular result shows that, even though we are using a partially coherent seed, the initial modulation across the pump possesses sufficient amplitude stability to strongly influence the pump dynamics. To understand this physically, it is instructive to compare the coherence time of the seed with the pump pulse duration. For an ASE seed with bandwidth $\Delta\lambda$, we can calculate the coherence time from $\tau_c = \lambda^2\ (c\Delta\lambda)^{-1}$ where c is the speed of light. Using our parameters with an ASE seed at $\lambda =$ 1531 nm with a 1 nm bandwidth, we find that the coherence time of $\tau_c \sim 8$ ps is longer than the input pulse. A strong effect from seeding is thus not surprising as the phase of the induced modulation would be expected to be stable across each pump pulse.

This interpretation is highly significant as it suggests that with broader ASE bandwidths (thus reduced coherence time), the influence of the low amplitude seed in the MI dynamics should decrease. This was then carefully investigated through additional experiments using the filtering setup to increase the ASE bandwidth over the range 1–36 nm (i.e., a decrease in coherence time from 8 to 0.21 ps). The results are shown in Fig. 4 and compared with numerical simulations. As expected, both the simulations and experiment show a steady decrease in the bandwidth and noise reduction for shorter coherence times. Such decrease is particularly striking as the ASE seed coherence time becomes significantly shorter than the pump pulse duration. For example, with ASE seed bandwidth of 36 nm, the corresponding coherence time is 0.2 ps and thus more than 10 times smaller than the 3.8 ps pump duration. We expect in this case a highly unstable initial modulation and would anticipate that the seed would have little effect. Indeed, for this case we see MI bandwidth and C_v of 76 nm and 0.75 respectively, close to the values observed in the absence of any seed. Differences between experiments and simulations are attributed to the fact that our noise model in the simulations does not completely reproduce the experimental noise on the pump or seed.

In conclusion, we have investigated the influence of a low amplitude partially coherent ASE seed on the bandwidth and noise properties of picosecond MI in a highly nonlinear fiber. By sweeping the ASE seed wavelength across the MI gain spectrum, significant increase in the spectral bandwidth is observed with maximum broadening observed when the seed coincides with the maximum of the MI gain. Real-time measurements performed using dispersive time stretching reveal a corresponding improvement in the noise properties. Experiments varying the ASE bandwidth further show that the influence of the ASE seed is only observed when its associated coherence time exceeds or is of the same order of magnitude as the pump pulses' duration. Our results suggest that resonant ASE seeding can provide an important tool in controlling the spectral properties of MI, and this may impact studies related to fiber source development where high-power pump sources are used to generate broadband SC light. In such cases, spectral filtering of any ASE pump could provide a complementary technique to modify the SC properties.

This work was supported by the European Research Council (ERC) Advanced Grant ERC-2011-AdG-290562 MULTIWAVE, the Agence Nationale de la Recherche (ANR OPTIROC), and the Air Force Office of Scientific Research, grant No. FA8655-13-1-2137.

DISTRIBUTION A. Approved for public release: distribution unlimited.

References

1. K. Tai, A. Hasegawa, and A. Tomita, Phys. Rev. Lett. **56**, 135 (1986).
2. E. J. Greer, D. M. Patrick, P. G. J. Wigley, and J. R. Taylor, Electron. Lett. **25**, 1246 (1989).
3. G. P. Agrawal, *Nonlinear Fiber Optics*, 5th ed. (Academic, 2012).
4. D. R. Solli, C. Ropers, P. Koonath, and B. Jalali, Nature **450**, 1054 (2007).
5. B. Kibler, J. Fatome, C. Finot, G. Millot, G. Genty, B. Wetzel, N. Akhmediev, F. Dias, and J. M. Dudley, Sci. Rep. **2**, 463 (2012).
6. G. Genty and J. M. Dudley, IEEE J. Quantum Electron. **45**, 1331 (2009).
7. G. Genty, J. M. Dudley, and B. J. Eggleton, Appl. Phys. B **94**, 187 (2009).
8. S. T. Sørensen, C. Larsen, U. Møller, P. M. Moselund, C. L. Thomsen, and O. Bang, J. Opt. Soc. Am. B **29**, 2875 (2012).
9. Q. Li, F. Li, K. K. Y. Wong, A. P. T. Lau, K. K. Tsia, and P. K. A. Wai, Opt. Express **19**, 13757 (2011).
10. D. R. Solli, C. Ropers, and B. Jalali, Phys. Rev. Lett. **101**, 233902 (2008).
11. K. K. Y. Cheung, C. Zhang, Y. Zhou, K. K. Y. Wong, and K. K. Tsia, Opt. Lett. **36**, 160 (2011).
12. D. Kip, M. Soljacic, M. Segev, E. Eugenieva, and D. N. Christodoulides, Science **290**, 495 (2000).
13. D. V. Dylov and J. W. Fleischer, Opt. Lett. **35**, 2149 (2010).
14. Z. Chen, J. Klinger, and D. N. Christodoulides, Phys. Rev. E **66**, 066601 (2002).
15. B. Wetzel, A. Stefani, L. Larger, P. A. Lacourt, J. M. Merolla, T. Sylvestre, A. Kudlinski, A. Mussot, G. Genty, F. Dias, and J. M. Dudley, Sci. Rep. **2**, 882 (2012).
16. D. R. Solli, G. Herink, B. Jalali, and C. Ropers, Nat. Photonics **6**, 463 (2012).
17. T. Godin, B. Wetzel, T. Sylvestre, L. Larger, A. Kudlinski, A. Mussot, A. Ben Salem, M. Zghal, G. Genty, F. Dias, and J. M. Dudley, Opt. Express **21**, 18452 (2013).
18. P. D. Drummond and J. F. Corney, J. Opt. Soc. Am. B **18**, 139 (2001).

DISTRIBUTION A. Approved for public release: distribution unlimited.

Ultrafast Single-Shot Measurements in Modulation Instability and Supercontinuum

The real-time measurement of ultrafast noisy processes is challenging because it requires single-shot resolution, broadband fidelity and long-record length. It is especially difficult to measure fluctuations in the optical supercontinuum, a white light source that can span over an octave in bandwidth. Yet, understanding noise in supercontinuum light and the intertwined process of modulation instability (MI) is critical. MI itself is one of the most fundamental processes in nonlinear physics, while supercontinuum noise studies yield new insights into the emergence of rogue wave events in settings from hydrodynamics to cold atoms.[1]

We studied shot-to-shot variations in both MI and supercontinuum generation using the time-stretch dispersive Fourier transform (TS-DFT) technique.[2–5] In TS-DFT, the intensity of a temporal field evolves into its Fourier transform with sufficient linear dispersive propagation, analogous to spatial far-field diffraction. Pulses from a mode-locked laser injected into a high-dispersion optical fiber are ultimately stretched such that their intensity profile matches their spectral envelope. Since this waveform is slow enough to be within the bandwidth of a real-time digitizer, it is possible to directly measure a series of single-shot spectra at the full laser repetition rate.

These measurements have uncovered new physics since access to large times-series permits detailed statistical analysis.[2,3,5] Experiments have shown that MI amplifies individual modes normally unseen in time-averaged experiments, lending insight into how patterns arise in other systems such as sand dunes.[2] Studies have also characterized supercontinuum noise around 1,550 nm and over an octave of bandwidth from 600–1,200 nm.[3,4] Extending TS-DFT to work across an octave required custom-fiber fabrication for the time-stretching step.[4] The correlation functions we calculated from experimental data revealed direct evidence of physical coupling between separated wavelength components, and the nature of the coupling was readily inferred from the correlation structure.[2,3]

Real-time measurements can expose hidden phenomena and yield insight into noise-driven nonlinear systems. More information remains to be unearthed from the libraries of single-shot spectra acquired by these means. OPN

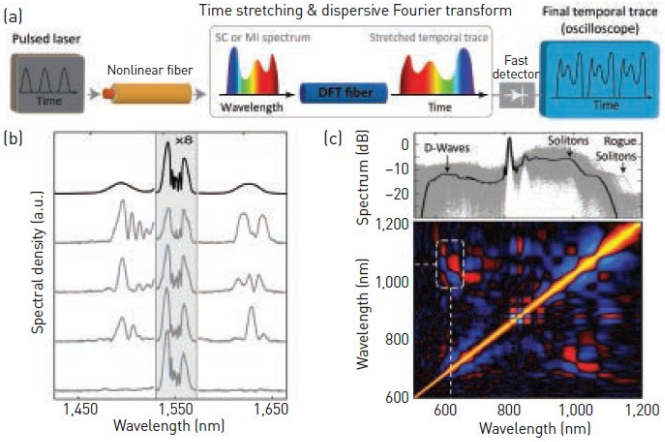

(a) Experimental setup. (b) Single-shot (gray) and average (black) MI spectra.[2] (c) Top: single-shot (gray) and average (black) supercontinuum spectra;[4] Bottom: correlation between solitons and dispersive waves 400 nm apart. Red (+), blue (-) and black (uncorrelated).

Researchers

Thomas Godin, **Benjamin Wetzel** and **John M. Dudley** (john.dudley@univ-fcomte.fr)
University of Franche-Comté, France

Georg Herink
University of Göttingen, Germany

Frédéric Dias
University College Dublin, Ireland

Goëry Genty
Tampere University of Tech., Finland

Bahram Jalali
University of Calif., Los Angeles, U.S.A.

Claus Ropers and **Daniel R. Solli**
University of Göttingen and University of Calif., Los Angeles

References

1. D.R. Solli et al. Nature **450**, 1054 (2007).
2. D.R. Solli et al. Nat. Photon. **6**, 463 (2012).
3. B. Wetzel et al. Scientific Rep. **2**, 882 (2012).
4. T. Godin et al. Opt. Express **21**, 18452 (2013).
5. D.R. Solli et al. Nonlinearity **26**, R85 (2013).

DISTRIBUTION A. Approved for public release: distribution unlimited.

Mid-IR parametric frequency generation in hybrid As_2Se_3 microwires using normal dispersion modulation instability

Thomas Godin[1], Yves Combes[1], Raja Ahmad[2], Martin Rochette[2], Thibaut Sylvestre[1], and John M. Dudley[1]
[1]*Institut FEMTO-ST, UMR 6174 CNRS-Université de Franche-Comté, Besançon, France*
[2]*Department of Electrical and Computer Engineering, McGill University, Montreal (QC) H3A 2A7, Canada*
thomas.godin@femto-st.fr

Abstract: We report the observation of modulation instability in the mid-infrared by pumping chalcogenide-polymer optical microwires in the normal dispersion regime. Modulation instability is allowed via negative fourth-order dispersion and leads to far-detuned parametric frequency conversion.
OCIS codes: (190.4370) Nonlinear optics, fibers, (190.4410) Nonlinear optics, parametric processes, (190.4380) Nonlinear optics, four-wave mixing, (320.7140) Ultrafast processes in fibers

1. Introduction

Chalcogenide glasses have emerged as extremely attractive materials for mid-infrared applications due to their striking optical properties such as broad IR transparency and high nonlinearities compared to silica [1]. There is therefore a still-growing interest in using chalcogenide glasses, such as As_2Se_3 or As_2S_3, in the frame of mid-IR supercontinuum (SC) generation, sensing, four-wave mixing or stimulated scatterings [2-4]. However, only little attention has been paid to the fundamental nonlinear process of spontaneous modulation instability (MI) in chalcogenide, which is associated with the exponential amplification of low amplitude noise on a continuous (or quasi-CW) pump wave. MI causes a significant temporal modulation of the pump and leads to the growth of symmetric sidebands on the spectrum. Noise-driven MI is thus a ubiquitous fundamental process in nonlinear physics as it is a key mechanism in fiber SC generation but also because of similarities with rogue instabilities in hydrodynamics [5]. It is usually considered that scalar MI requires pumping in the anomalous dispersion regime to satisfy the phase-matching conditions. However, these conditions can also be satisfied in the normal dispersion regime provided the waveguide possesses a suitable higher-order group velocity dispersion profile, as shown for instance by *Harvey et al.* in a silica photonic crystal fiber [6]. We report here the observation of far-detuned broadband frequency conversion due to normal dispersion MI in a highly-nonlinear hybrid As_2Se_3-polymer tapered optical fiber with dispersion profile allowing phase-matched frequency conversion through fourth-order dispersion.

2. Experimental and numerical results

The experimental setup is shown in Fig. 1(a) along with a schematic of the As_2Se_3 microwire. The input core size in the untapered region is 16 µm and is reduced down to 3.6 µm in the 14-cm long uniform tapered region, corresponding to a zero-dispersion wavelength of 2830 nm.

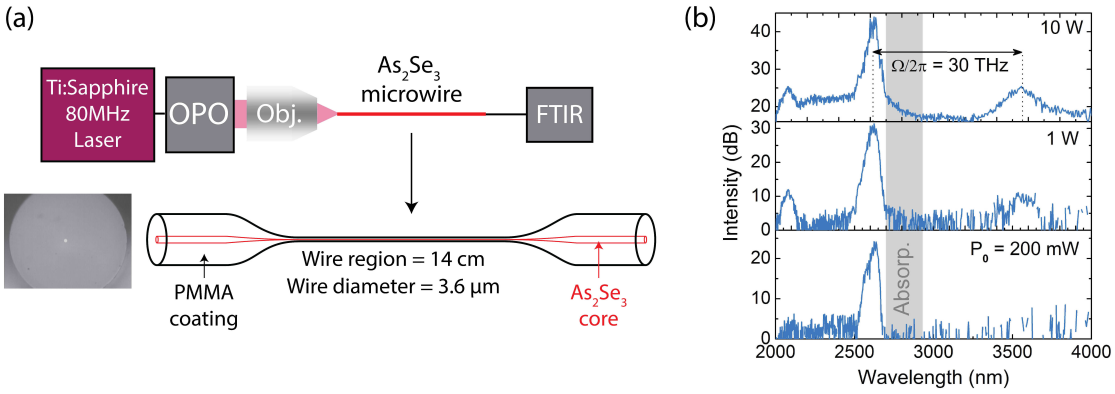

Fig. 1 (a) Experimental setup. OPO: Optical Parametric Oscillator. FTIR: Fourier-transform infrared spectrometer. Inset: wire input facet (b) Experimental observation of modulation instability when pumping at λ = 2620 nm in the normal dispersion regime. The zero-dispersion wavelength is located at λ = 2830 nm. The shaded area represents the OH absorption band.

DISTRIBUTION A. Approved for public release: distribution unlimited.

By pumping in the normal dispersion regime at 2620 nm with ~600 fs pulses from an optical parametric oscillator and increasing pump powers, we thus obtained the spectra shown in Fig. 2(b). We observe the clear emergence of two widely spaced MI sidebands, symmetric in frequency, with the short-wavelength sideband centered at 2080 nm and the long-wavelength at 3555 nm, corresponding to a frequency shift $\Omega/2\pi = \pm 30$ THz. This is the largest frequency shift reported using normal dispersion MI in a single-pass configuration and in spite of the presence of an OH absorption band located around 2.75 µm inducing losses of ~13 dB.m^{-1}. At the pump wavelength, the phase-matched frequency conversion process is allowed by a positive second-order dispersion ($\beta_2 = 2.9296 \times 10^{-2}$ ps^2 m^{-1}) mediated by negative fourth-order dispersion ($\beta_4 = -9.89\times10^{-6}$ ps^4 m^{-1}).

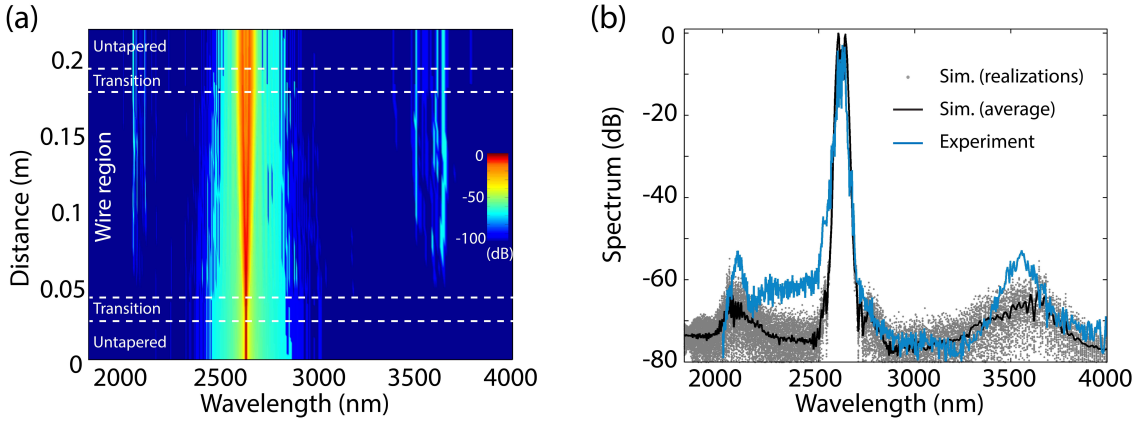

Fig. 2 (a) Spectral evolution simulated along the 22 cm microwire length showing the dynamics of normal dispersion MI. (b) Simulated results showing mean spectrum at the microwire output (black) compared with experiment (cyan). Individual realizations from the ensemble of 250 shot-to-shot spectra are also shown (gray dots).

The 30 THz frequency shift has been confirmed by calculating the parametric gain using a standard stability analysis approach. We also performed numerical simulations based on a stochastic nonlinear Schrödinger equation model including variations in nonlinear and dispersion parameters along the microwire length and a stochastic noise model. Kerr and delayed Raman contributions were also taken into account. Figure 2(a) shows the pulse propagation in the different segments of the microwire and we notice that the sidebands generation is initiated in the wire region, where nonlinear properties are enhanced. Output spectra have been calculated from an ensemble of 250 realizations and are in good agreement with experimental measurements, as shown in Fig. 2(b).

In conclusion, we have demonstrated a mid-infrared parametric frequency converter based on normal dispersion pumped scalar MI with 1.5 µm wavelength spacing. These results highlight the great potential of chalcogenide microwires for applications in the mid-IR ranging from absorption spectroscopy to entangled photon pairs generation.

The authors acknowledge the support the European Research Council (ERC) Advanced Grant ERC-2011-AdG-290562 MULTIWAVE, the Agence Nationale de la Recherche (ANR OPTIROC), the Air Force Office of Scientific Research grant number FA8655-13-1-2137, and the Natural Science and Engineering Research council of Canada (NSERC).

3. References

[1] B. J. Eggleton, B. Luther-Davies, and K. Richardson, "Chalcogenide photonics", Nat. Photon. **5**, 141-148 (2011).
[2] A. Al-kadry, C. Baker, M. El Amraoui, Y. Messaddeq, And M. Rochette, "Broadband supercontinuum generation in As_2Se_3 chalcogenide wires by avoiding the two-photon absorption effects", Opt. Lett. **38**, 1185-1187 (2013).
[3] D. D. Hudson, S. A. Dekker, E.C. Mägi, A.C. Judge, S. D. Jackson, E. Li, J. S. Sanghera, L. B. Shaw, I. D. Aggarwal, and B. J. Eggleton, "Octave spanning supercontinuum in an As_2S_3 taper using ultralow pump pulse energy", Opt. Lett. **36**, 1122 (2011).
[4] J. C. Beugnot, R. Ahmad, M. Rochette, V. Laude, H. Maillotte, and T. Sylvestre, "Reduction and control of stimulated Brillouin scattering in polymer-coated chalcogenide optical microwires", Opt. Lett. **39**, 482-485 (2014).
[5] D. R. Solli, G. Herink, B. Jalali, and C. Ropers, "Fluctuations and correlations in modulation instability", Nat. Photon. **6**, 463-468 (2012).
[6] J. D. Harvey, R. Leonhardt, S. Coen, G. K. L. Wong, J. C. Knight, W. J. Wadsworth, and P. St. Russell, "Scalar modulation instability in the normal dispersion regime by use of a photonic crystal fiber", Opt. Lett. **28**, 2225-2227 (2003).

DISTRIBUTION A. Approved for public release: distribution unlimited.

Unexpected Ultrafast

New Frontiers in the Physics and Applications of Ultrafast Optics


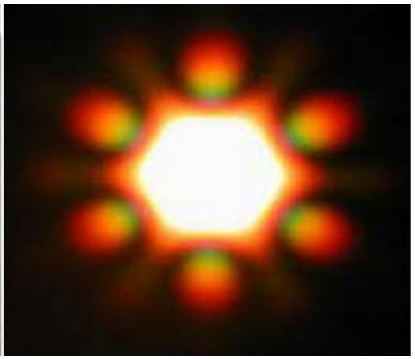


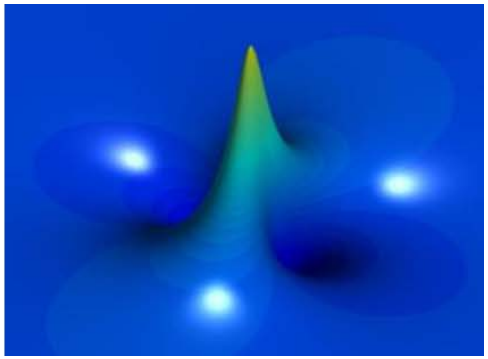

John Dudley
CNRS Institut FEMTO-ST
Université de Franche-Comté
Besançon, France
@johnmdudley

United Nations Educational, Scientific and Cultural Organization

International Year of Light 2015

DISTRIBUTION A. Approved for public release: distribution unlimited.

Summary

Ultrashort pulses of light are finding new and unexpected applications in many fields

Optical fibre supercontinuum

Shaped light for material processing

Toy models of physics

DISTRIBUTION A. Approved for public release: distribution unlimited.

Ultrashort pulses in optical fibres

DISTRIBUTION A. Approved for public release: distribution unlimited.

The history of the soliton

Glasgow-Paisley-Ardrossan Canal, Scotland 1835

Barges towed with v > 5 mph were observed to “sit” upon a bow wave

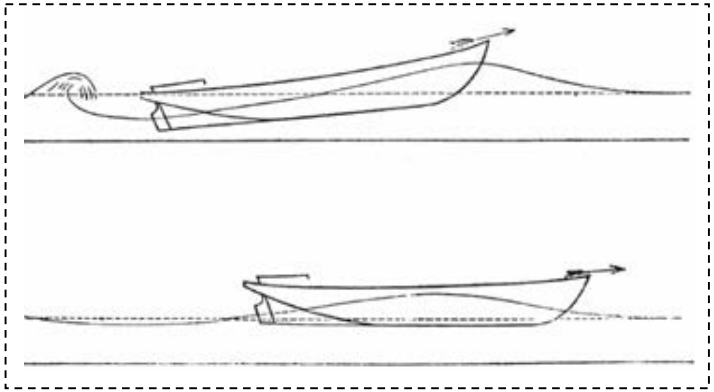

DISTRIBUTION A. Approved for public release: distribution unlimited.

Canal engineering in 19th century

1834: “The happiest day of my life”

John Scott Russell (1808-1882)
Engineer and entrepreneur

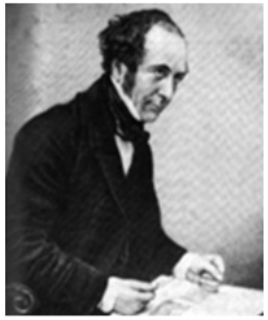

Systematic Studies in Edinburgh

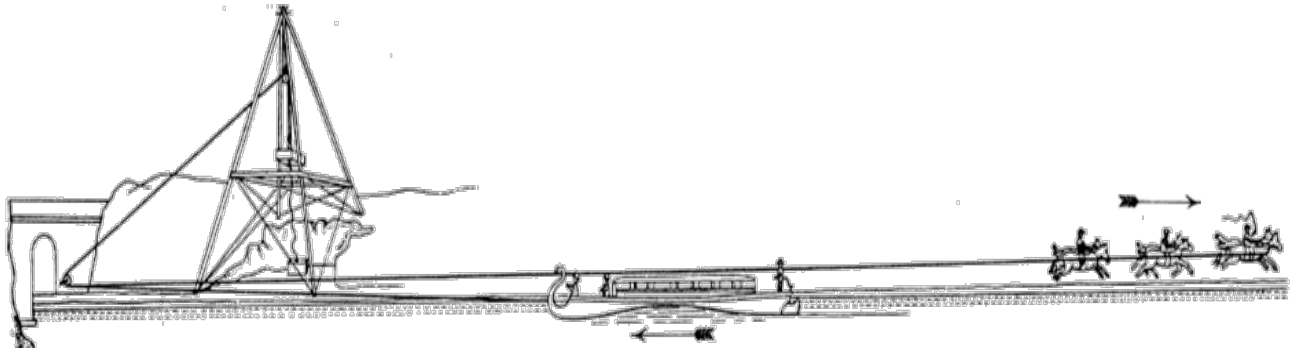

“the boat suddenly stopped –
not so the mass of water in the
channel which it had put in motion
…
a large, solitary, progressive wave”

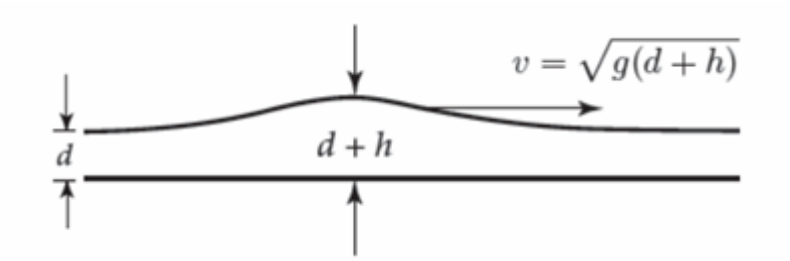

DISTRIBUTION A. Approved for public release: distribution unlimited.

Why this is unusual – a modern example with light

Light waves usually disperse (diffract) with propagation

Nonlinear self-compression (self-focussing) balances the usual linear tendency of a wave to disperse (or diffract)

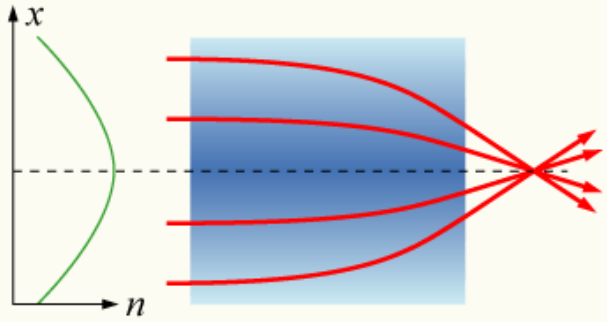

$I(x)$ $\quad n = n_0 + n_2\, I(x)$

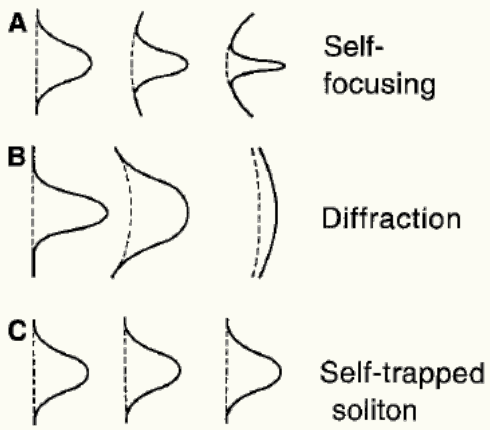

$\Delta n \sim n_2 I \sim 10^{-6}$ – small but dynamic & controllable !

Optical soliton - a structure of light where the balance between linear and nonlinear effects yields propagation that does not change

DISTRIBUTION A. Approved for public release: distribution unlimited.

Solitons in an ultrashort pulse laser

42 OPTICS LETTERS / Vol. 16, No. 1 / January 1, 1991

60-fsec pulse generation from a self-mode-locked Ti:sapphire laser

D. E. Spence, P. N. Kean, and W. Sibbett

Femtosecond Ti:Sapphire laser, the heart of the femtosecond laser frequency comb

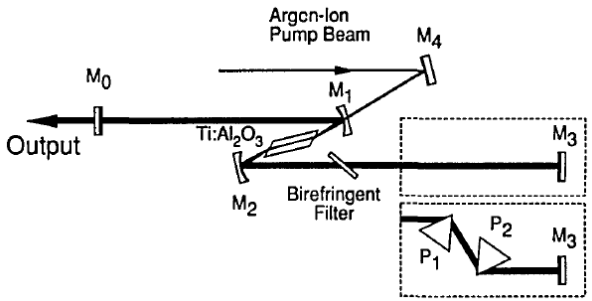

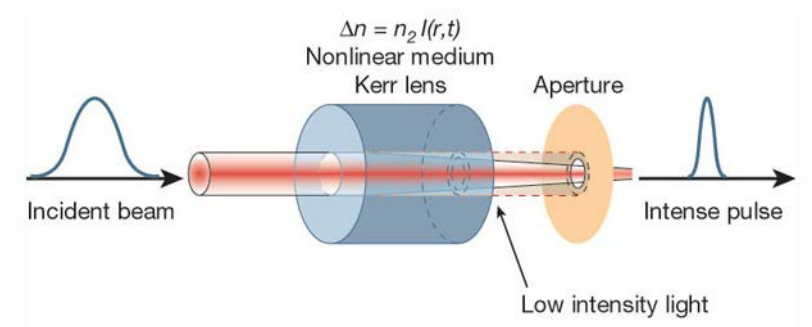

Temporal solitons

Spatial solitons

DISTRIBUTION A. Approved for public release: distribution unlimited.

Dispersion management

Diffraction management

Low-loss optical waveguide development

Reliable techniques for fabricating small-core waveguides allows tailored linear guidance (dispersion) and controlled nonlinear interactions

PROC. IEE, Vol. 113, No. 7, JULY 1966

Dielectric-fibre surface waveguides for optical frequencies

K. C. Kao, B.Sc.(Eng.), Ph.D., A.M.I.E.E., and G. A. Hockham, B.Sc.(Eng.), Graduate I.E.E.

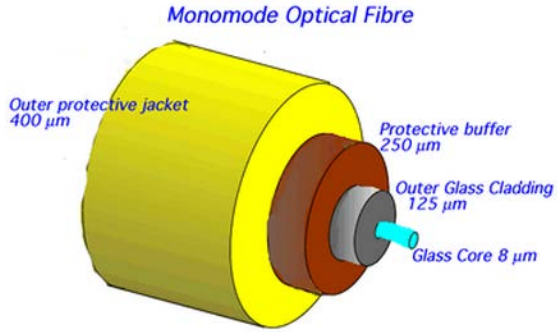

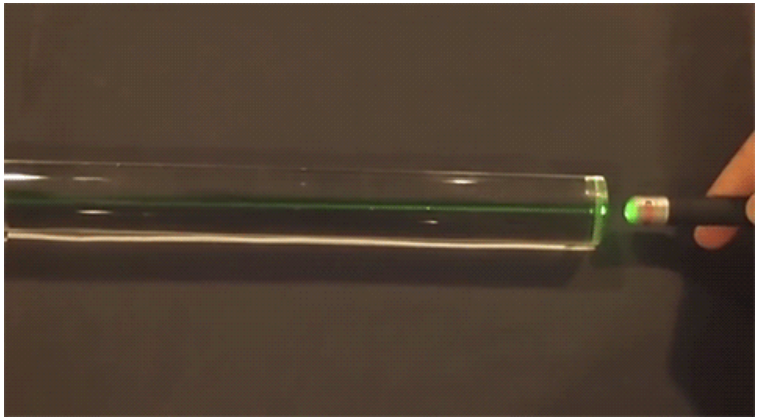

DISTRIBUTION A. Approved for public release: distribution unlimited.

Low-loss optical waveguide development

Reliable techniques for fabricating small-core waveguides allows tailored linear guidance (dispersion) and controlled nonlinear interactions

PROC. IEE, Vol. 113, No. 7, JULY 1966

Dielectric-fibre surface waveguides for optical frequencies

K. C. Kao, B.Sc.(Eng.), Ph.D., A.M.I.E.E., and G. A. Hockham, B.Sc.(Eng.), Graduate I.E.E.

United Nations Educational, Scientific and Cultural Organization

International Year of Light 2015

With such huge changes that optical fibres have made to lifestyles and wellbeing globally in these last fifty years, it is timely to celebrate all the consequences.

Gwen Kao, 2014

The Nobel Prize in Physics 2009

DISTRIBUTION A. Approved for public release: distribution unlimited.

A soliton laser injected into optical fibre

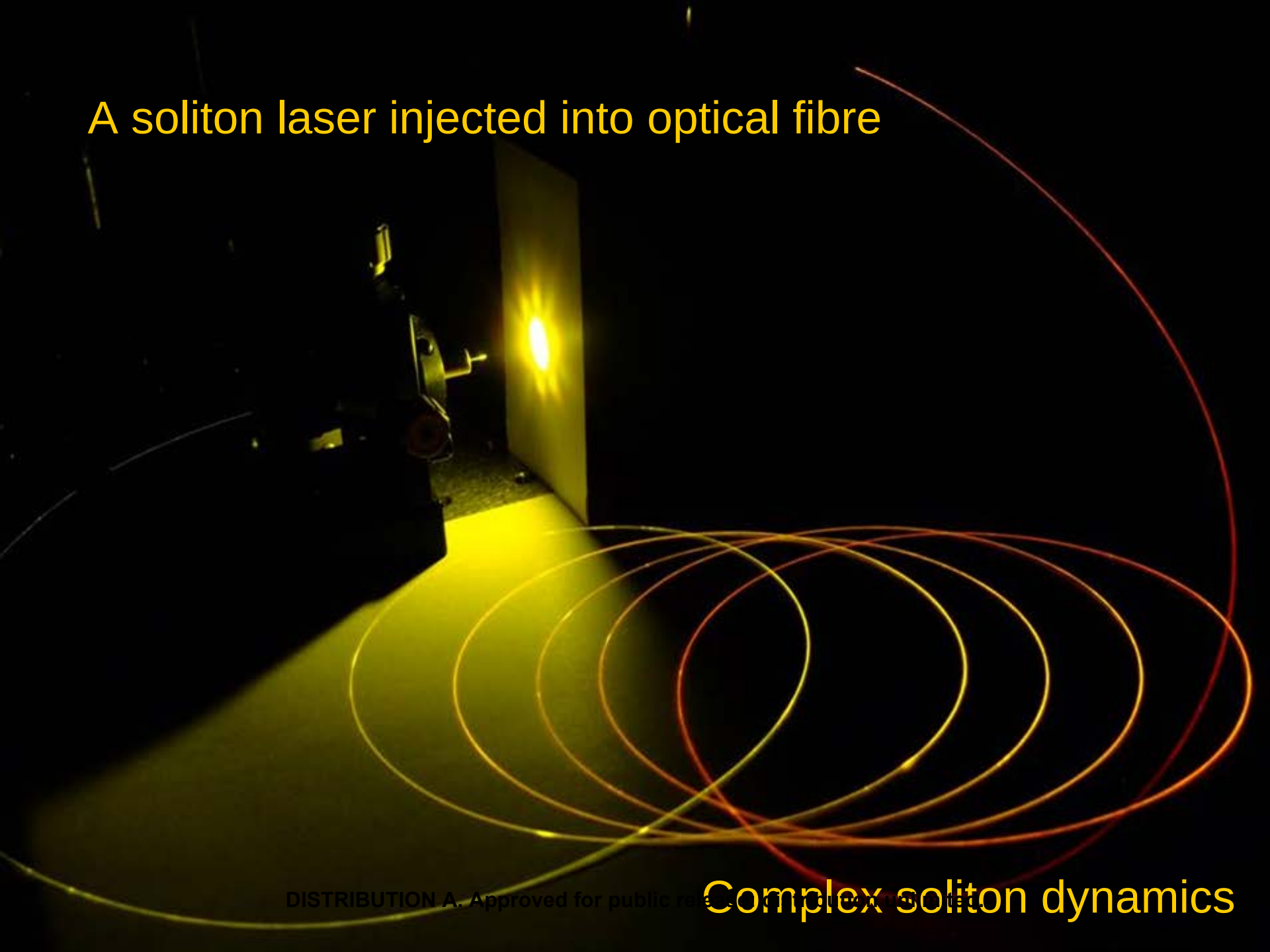

Complex soliton dynamics

DISTRIBUTION A. Approved for public release; distribution unlimited.

The optical frequency comb

Description of ultrashort pulses

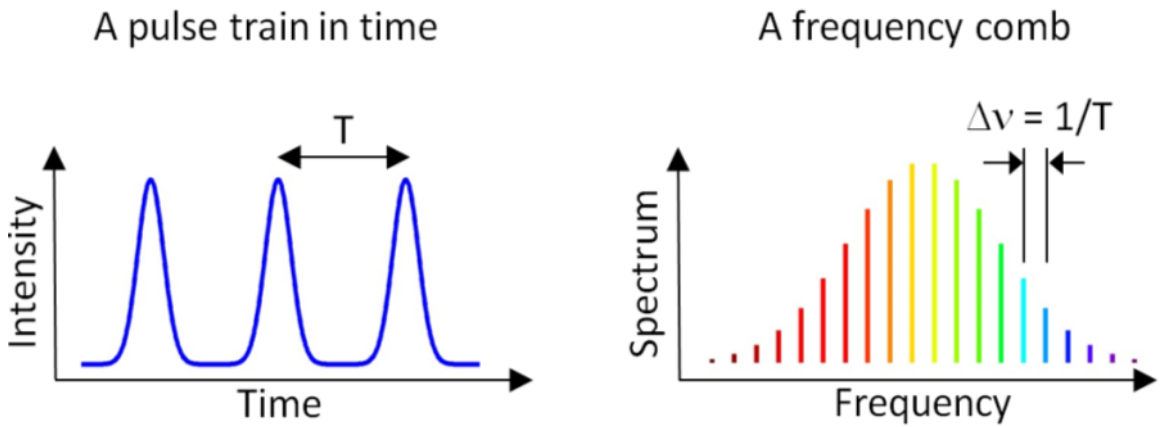

An octave-spanning spectrum allows comb position to be readily stabilized

We can bridge the gap between a known optical frequency locked to definition of the second and any optical frequency

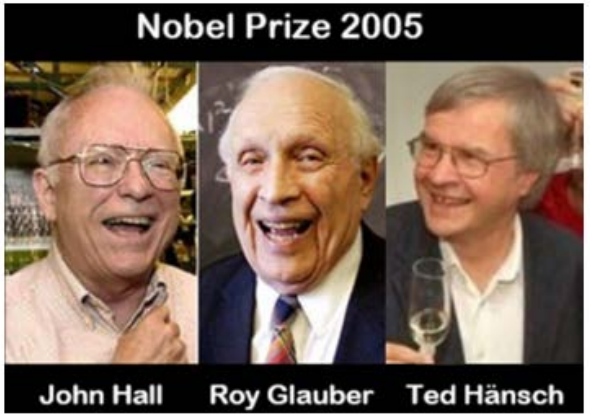

DISTRIBUTION A. Approved for public release: distribution unlimited.

Many different applications

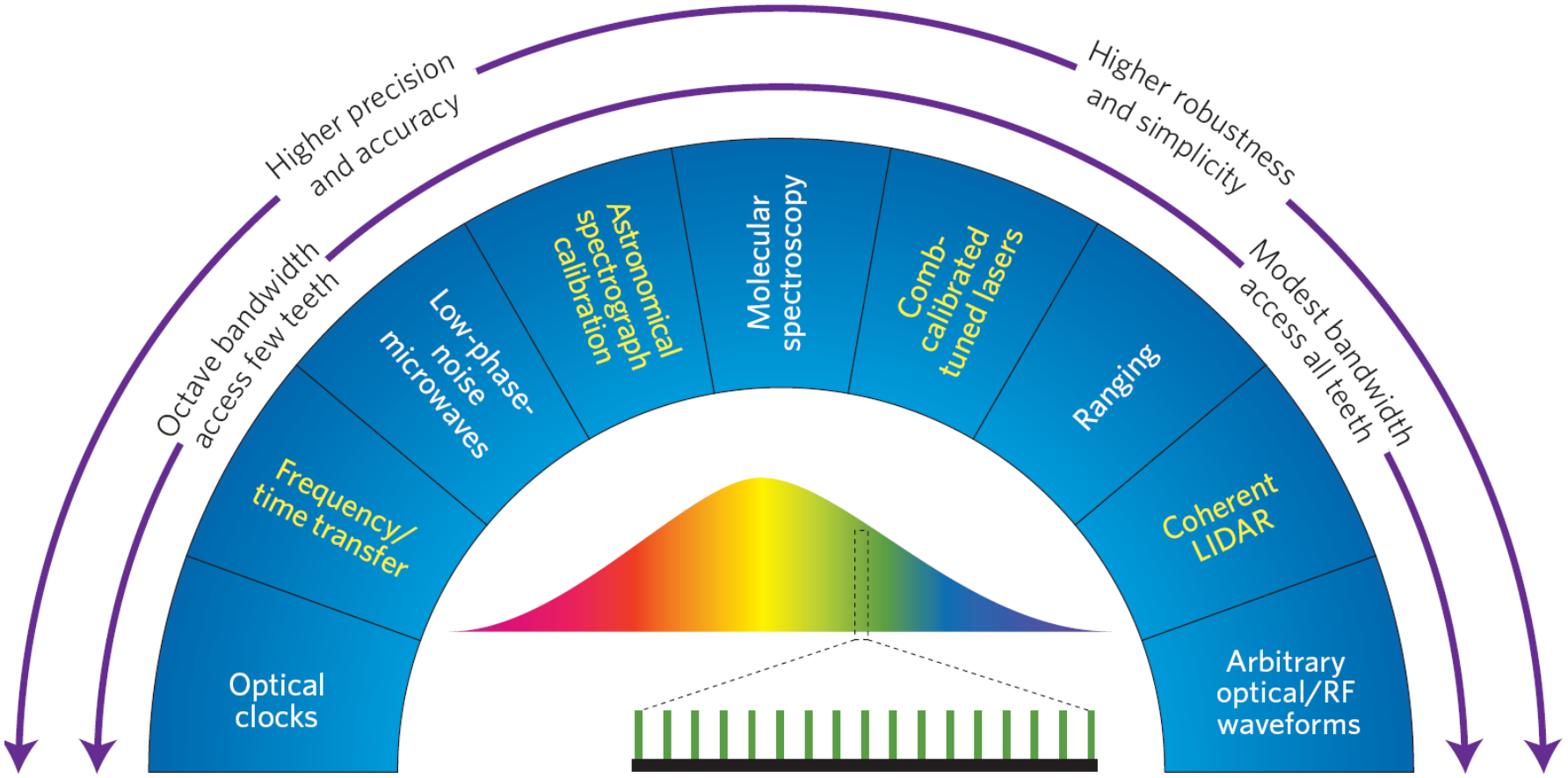

DISTRIBUTION A. Approved for public release: distribution unlimited.

Example: broadband light source

Molecular fingerprinting — S. Diddams *et al.* Nature **445**, 627 (2007)
Human breath analysis — M. J. Thorpe *et al.* Opt. Express **16**, 2387 (2008)

nature photonics | VOL 2 | JANUARY 2008 | www.nature.com/naturephotonics

INDUSTRY PERSPECTIVE | TECHNOLOGY FOCUS

METROLOGY

Broad as a lamp, bright as a laser

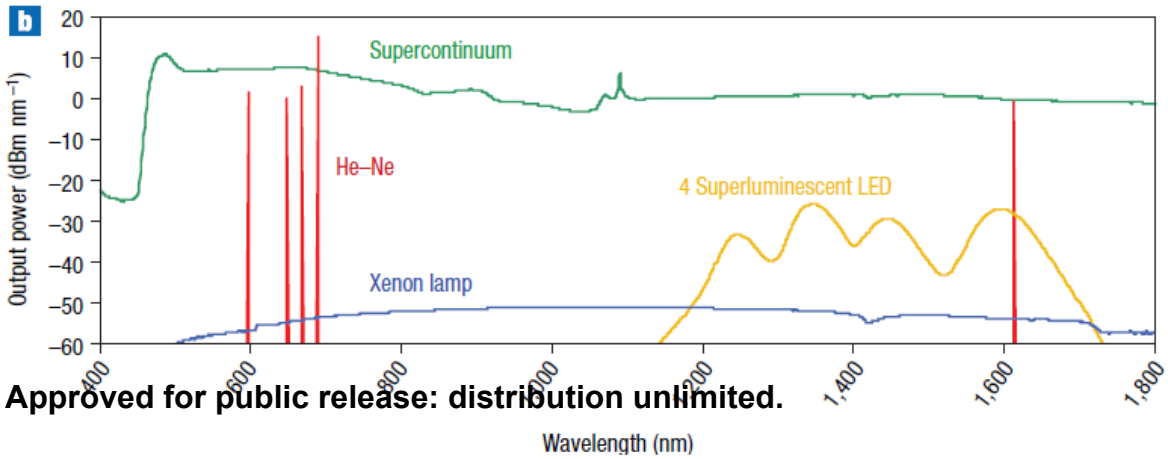

DISTRIBUTION A. Approved for public release: distribution unlimited.

Working with new materials

nature photonics
FOCUS | REVIEW ARTICLES
PUBLISHED ONLINE: 30 JULY 2010 | DOI: 10.1038/NPHOTON.2010.185

Nonlinear silicon photonics

J. Leuthold*, C. Koos and W. Freude

Silicon offers an abundance of nonlinear optical effects that can be used to generate and process optical signals in low-cost ultracompact chips at speeds beyond those of today's electronic devices. The Review discusses the nonlinear optical effects in silicon and highlights some of the associated key applications.

nature photonics
REVIEW ARTICLE
PUBLISHED ONLINE: 28 FEBRUARY 2011 | DOI: 10.1038/NPHOTON.2011.309

Chalcogenide photonics

Benjamin J. Eggleton[1]*, Barry Luther-Davies[2] and Kathleen Richardson[3]

The unique and striking material properties of chalcogenide glasses have been studied for decades, providing applications ir the electronics industry, imaging and more recently in photonics. This Review summarizes progress in photonic devices that exploit the unique optical properties of chalcogenide glasses for a range of important applications, focusing on recent examples in mid-infrared sensing, integrated optics and ultrahigh-bandwidth signal processing.

Material	Nonlinear index*	Nonlinear absorption
Chalcogenide glass	100 to 500	Low to moderate
Bismuth Oxide	55	Low
Silicon	170	High
Silica	1	Low

*Relative to silica ($n_2 = 2.6 \times 10^{-20}$ m^2/W)

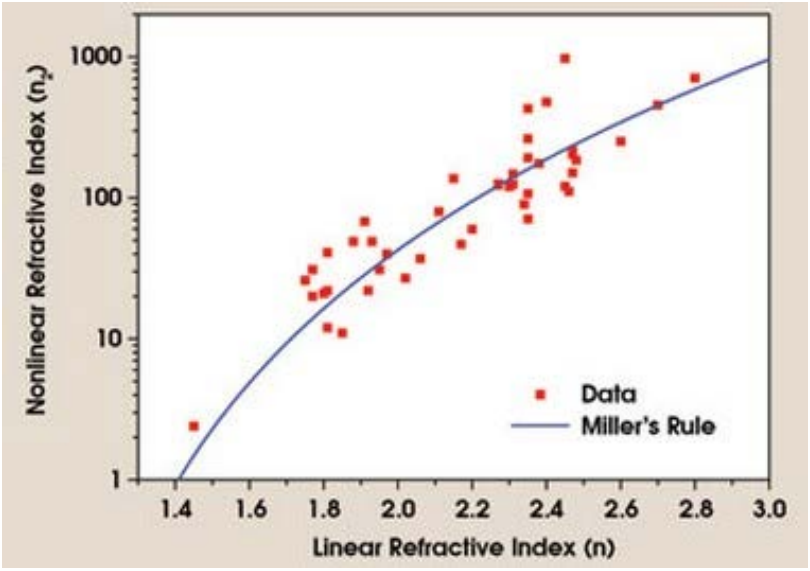

DISTRIBUTION A. Approved for public release: distribution unlimited.

Mid-infrared photonics

LETTERS
PUBLISHED ONLINE: 14 SEPTEMBER 2014 | DOI: 10.1038/NPHOTON.2014.213
nature photonics

Mid-infrared supercontinuum covering the 1.4–13.3 μm molecular fingerprint region using ultra-high NA chalcogenide step-index fibre

Christian Rosenberg Petersen[1]*, Uffe Møller[1], Irnis Kubat[1], Binbin Zhou[1], Sune Dupont[2], Jacob Ramsay[2], Trevor Benson[3], Slawomir Sujecki[3], Nabil Abdel-Moneim[3], Zhuoqi Tang[3], David Furniss[3], Angela Seddon[3] and Ole Bang[1,4]

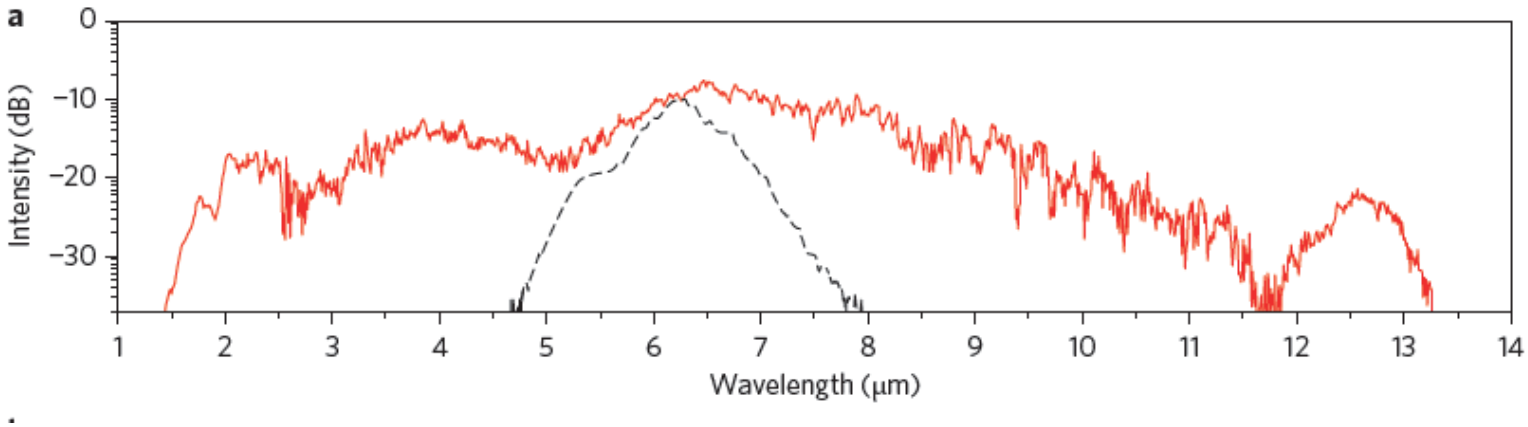

DISTRIBUTION A. Approved for public release: distribution unlimited.

Ultrashort pulses for material processing

DISTRIBUTION A. Approved for public release: distribution unlimited.

Femtosecond pulses & material processing

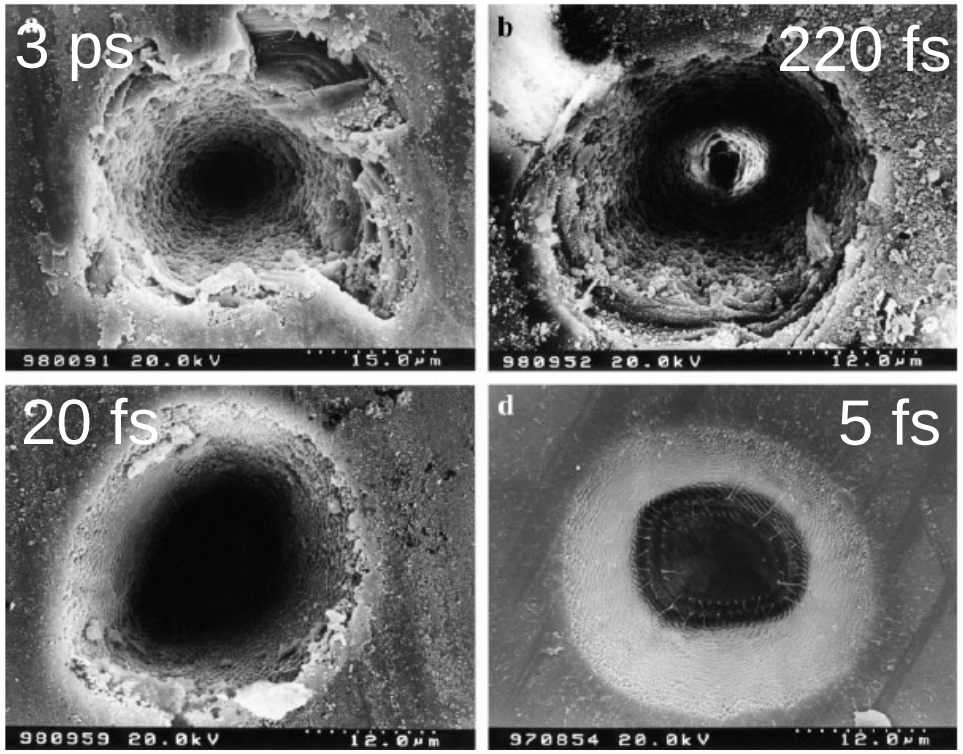

Reduced
thermal damage

Precision laser ablation of dielectrics in the 10-fs regime
M. Lenzner, J. Krüger, W.Kautek, F. Krausz, Wien, Austria

Appl. Phys. A 68, 369–371 (1999)

DISTRIBUTION A: Approved for public release: distribution unlimited.

Spatial structuring of a femtosecond laser beam

Gaussian beams have tradeoff between intensity and interaction length

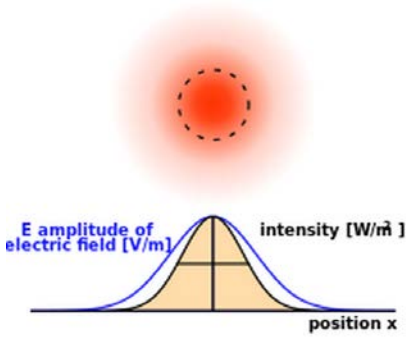

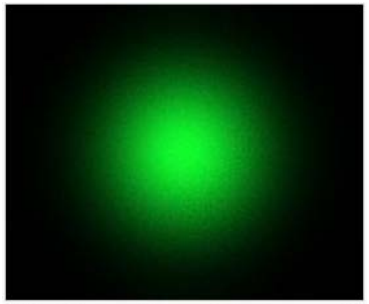

A 5 mW green laser pointer beam profile, showing the TEM_{00} profile

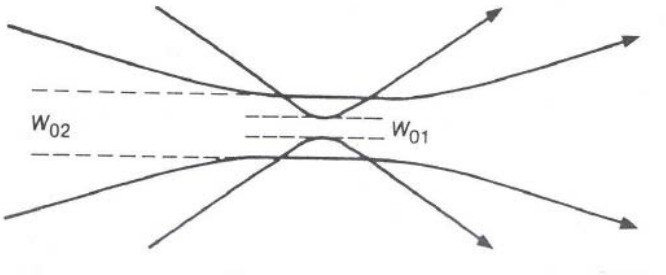

$$2z_{\mathrm{R}} = \frac{2\pi w_0^2}{\lambda}$$

DISTRIBUTION A. Approved for public release: distribution unlimited.

Transforming a laser beam to a more useful structure

Maxwell's equations admit other propagative solutions – Bessel beams

Axicon

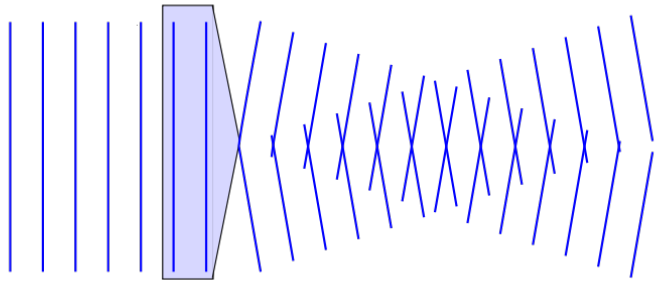

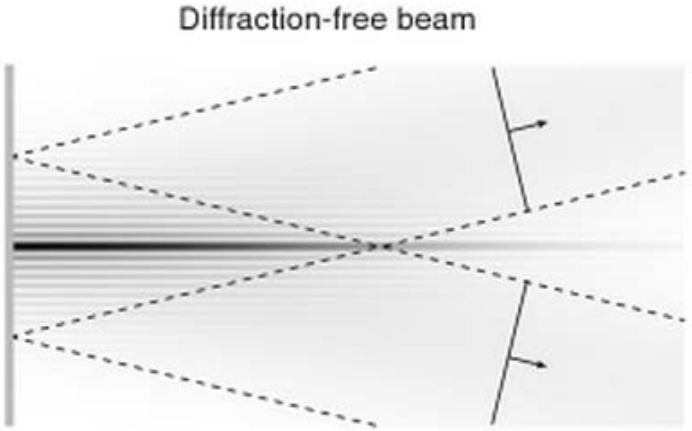

DISTRIBUTION A. Approved for public release: distribution unlimited.

Experimental synthesis

We impose the required spatial phase using a spatial light modulator and reduce it to nanometric dimensions using an imaging system

Convert femtosecond laser to have a Bessel beam profile

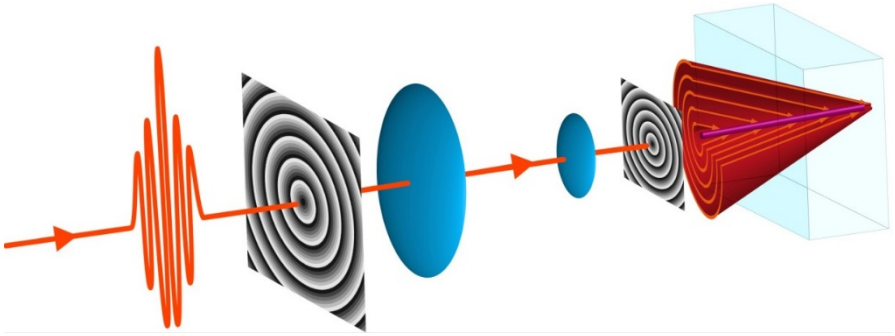

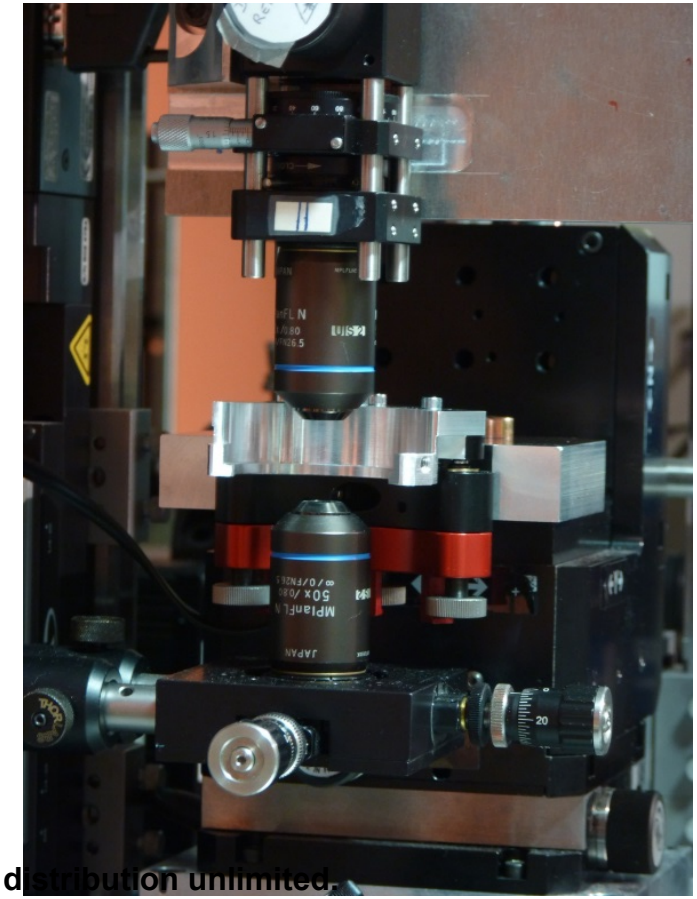

Another kind of nonlinear localisation

- stable filamentation

DISTRIBUTION A. Approved for public release: distribution unlimited.

Applications of Bessel beams

Superresolution machining

Threshold effect of ablation means that structure diameter is less than the beam diameter

fs pulses at 800 nm yield 200 nm channels

Fused silica

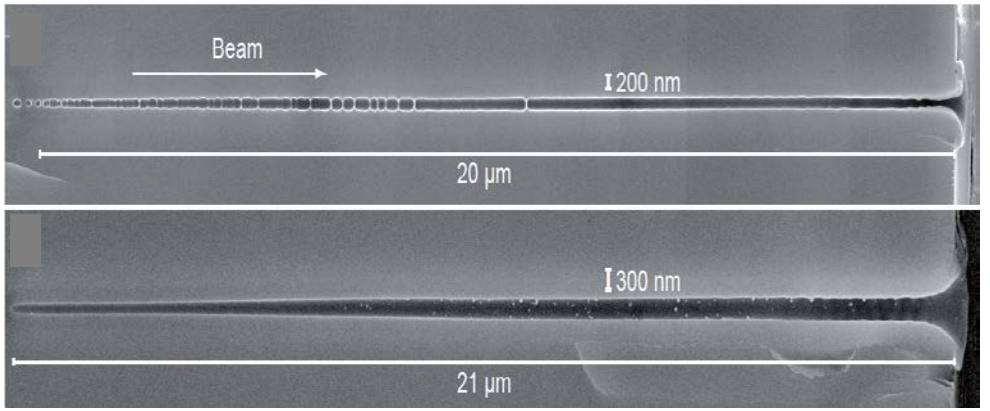

M. Bhuyan *et al.* Appl. Phys. Lett. **97** 081102 (2010)

Annular surface structures using vortex Bessel beams

Higher-order Bessel solutions offer possibilities for surface structuring

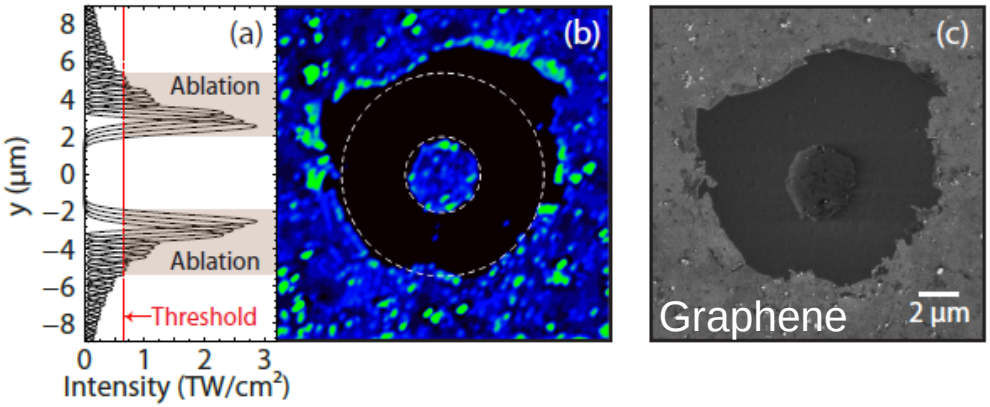

B. Wetzel *et al.* Appl. Phys. Lett., **103** 241111 (2013)

DISTRIBUTION A. Approved for public release: distribution unlimited.

Applications of Bessel beams

Superresolution machining

Threshold effect of ablation means that structure diameter is less than the beam diameter

fs pulses at 800 nm yield 200 nm channels

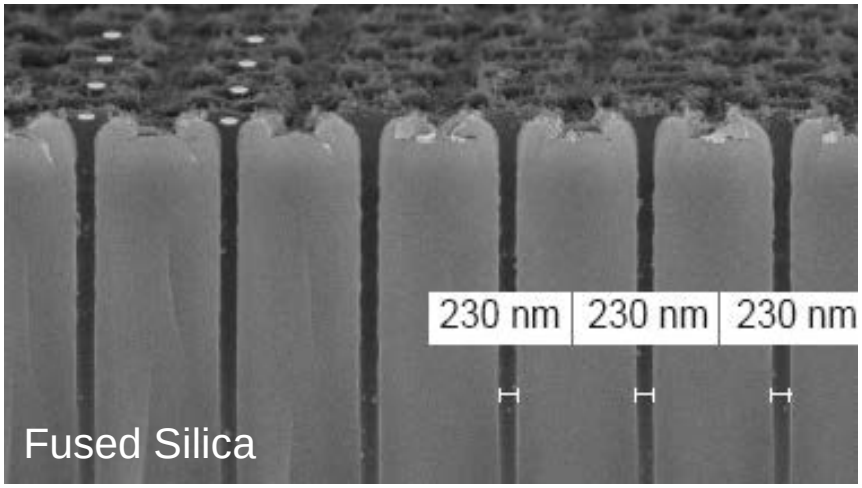

M. Bhuyan *et al.* Appl. Phys. Lett. **97** 081102 (2010)

Annular surface structures using vortex Bessel beams

Higher-order Bessel solutions offer possibilities for surface structuring

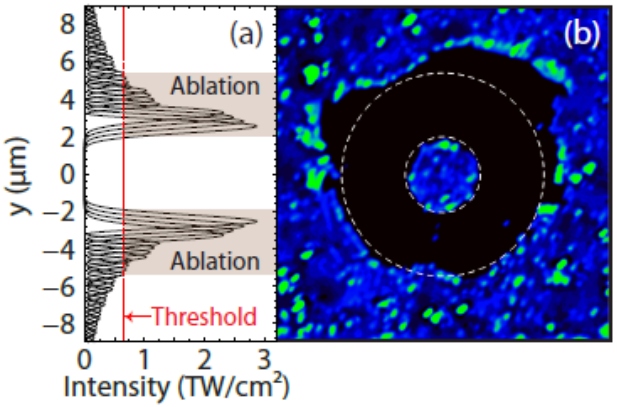

B. Wetzel *et al.* Appl. Phys. Lett., **103** 241111 (2013)

DISTRIBUTION A. Approved for public release: distribution unlimited.

Applications of Bessel beams

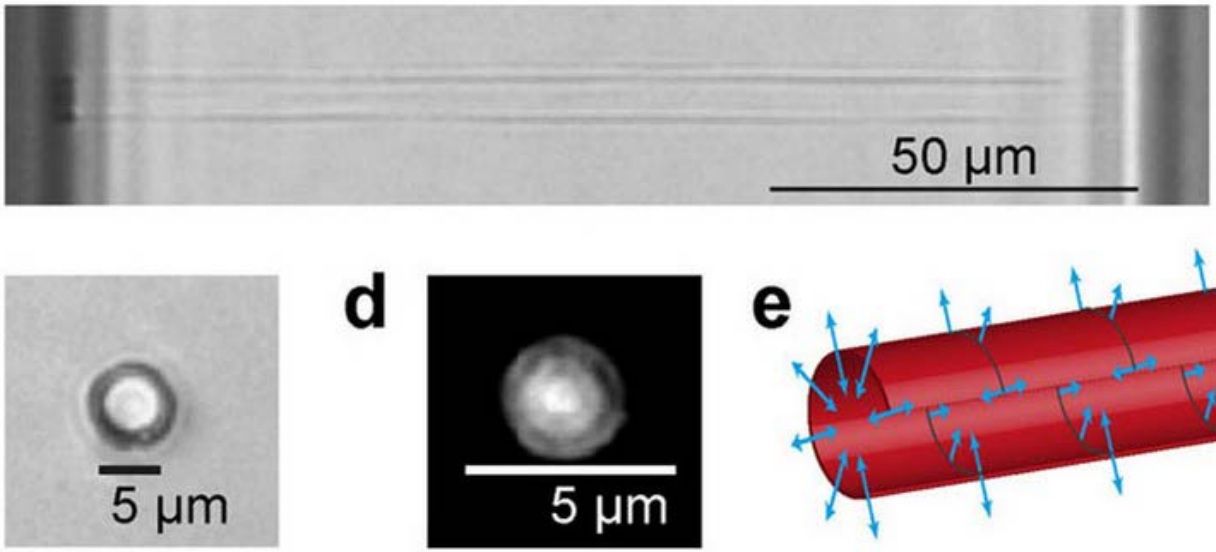

Annular volumetric structures using vortex Bessel beams

Higher-order Bessel solutions offer possibilities for surface structuring

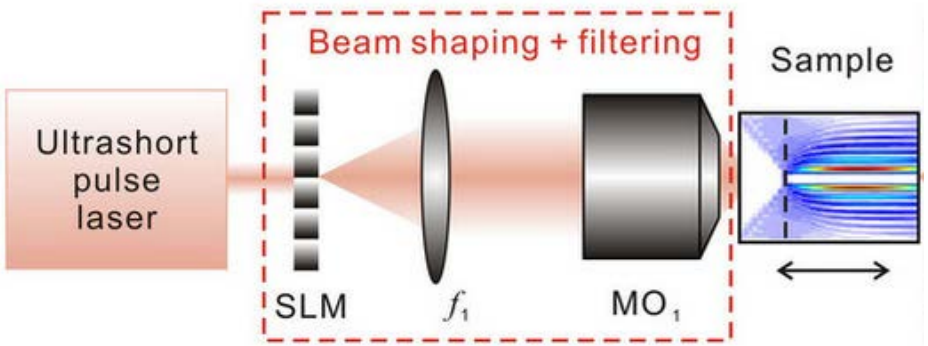

DISTRIBUTION A. Approved for public release: distribution unlimited.

Xie et al. Scientific Reports **5**, 8914 (2015)

Local intensity maxima need not travel in straight lines

Accelerating beams – intensity peaks follow caustics

264 Am. J. Phys. 47(3), Mar. 1979

Nonspreading wave packets

M. V. Berry
H. H. Wills Physics Laboratory, Tyndall Avenue, Bristol, BS8 1TL, United Kingdom

N. L. Balazs
State University of New York at Stony Brook, Stony Brook, New York 11794
(Received 30 June 1978; accepted 12 September 1978)

Fold catastrophe: Airy profile

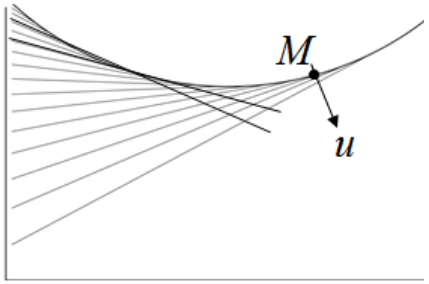

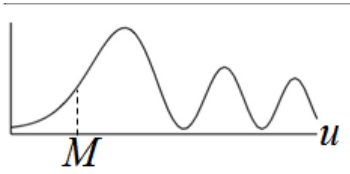

$$I_M(u) \approx \mathrm{Ai}^2\left[-\left(\frac{2k^2}{R(z)}\right)^{1/3} u\right]$$

Individual rays travel in straight lines,
it is the envelope that curves

DISTRIBUTION A. Approved for public release: distribution unlimited.

Applications of accelerating beams

APPLIED PHYSICS LETTERS **101**, 071110 (2012)

Micromachining along a curve: Femtosecond laser micromachining of curved profiles in diamond and silicon using accelerating beams

A. Mathis, F. Courvoisier,[a)] L. Froehly, L. Furfaro, M. Jacquot, P. A. Lacourt, and J. M. Dudley
Département d'Optique P.M. Duffieux, Institut FEMTO-ST, UMR 6174 CNRS Université de Franche-Comté, 25030 Besançon Cedex, France

(Received 4 July 2012; accepted 31 July 2012; published online 14 August 2012)

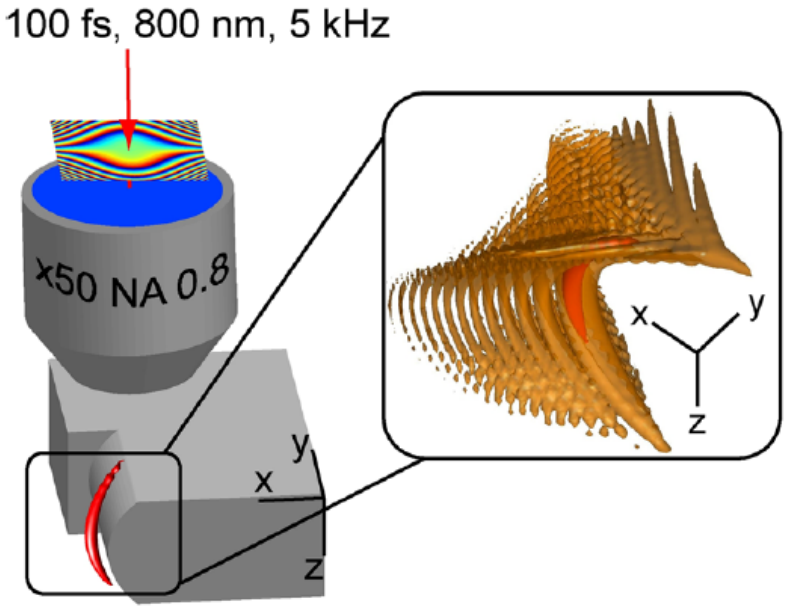

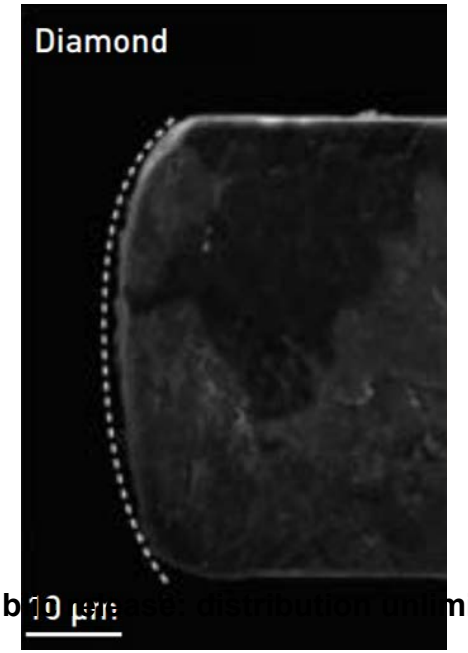

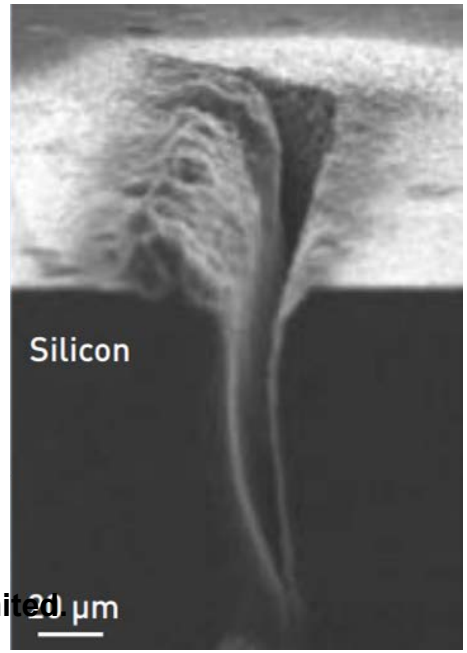

DISTRIBUTION A. Approved for public release; distribution unlimited.

Spherical Light

2218 OPTICS LETTERS / Vol. 38, No. 13 / July 1, 2013

Arbitrary nonparaxial accelerating periodic beams and spherical shaping of light

A. Mathis, F. Courvoisier,* R. Giust, L. Furfaro, M. Jacquot, L. Froehly, and J. M. Dudley
Département d'Optique P.M. Duffieux, Institut FEMTO-ST, UMR 6174 CNRS Université de Franche-Comté, 25030 Besançon cedex, France
**Corresponding author: francois.courvoisier@femto-st.fr*

Received April 11, 2013; revised May 24, 2013; accepted May 24, 2013;
posted May 29, 2013 (Doc. ID 188684); published June 21, 2013

We report the observation of arbitrary accelerating beams (ABs) designed using a nonparaxial description of optical caustics. We use a spatial light modulator-based setup and techniques of Fourier optics to generate circular and Weber beams subtending over 95 deg of arc. Applying a complementary binary mask also allows the generation of periodic ABs taking the forms of snake-like trajectories, and the application of a rotation to the caustic allows the first experimental synthesis of optical ABs upon the surface of a sphere in three dimensions. © 2013 Optical Society of America

OCIS codes: (350.5500) Propagation; (350.7420) Waves; (070.3185) Invariant optical fields; (070.7345) Wave propagation; (070.6120) Spatial light modulators; (260.1960) Diffraction theory.
http://dx.doi.org/10.1364/OL.38.002218

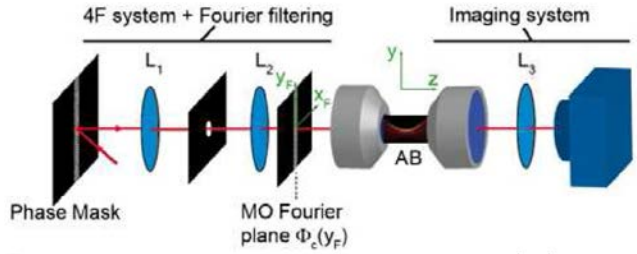

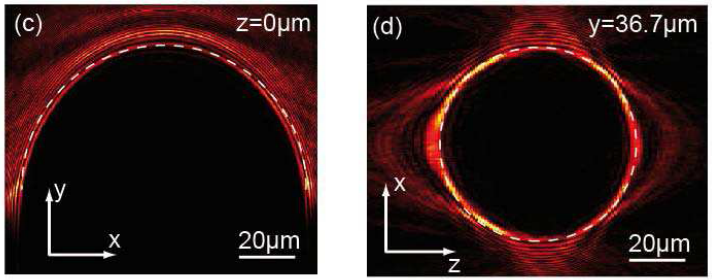

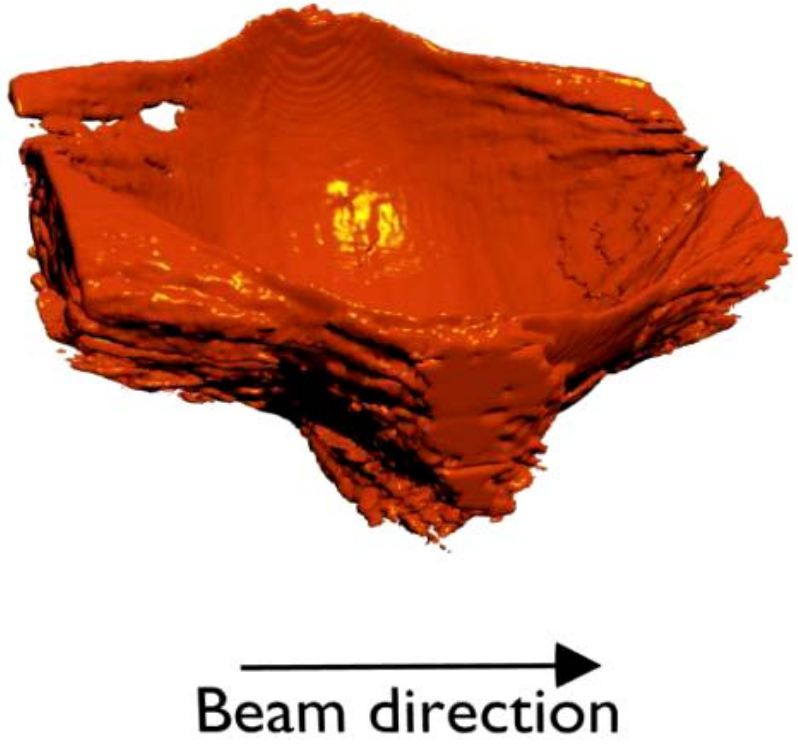

Fig. 4. (Media1) Experimental spherically shaped field. (a) and (b) 3D isointensity surfaces of the experimental beam at 30% of maximal intensity. Media1 shows rotation. Inset: rotation phase mask (unwrapped). (c) and (d) Cross-sections in xy and xz planes. White dashed lines show the cross sections of a 50 μm radius half-sphere. Scaling is identical in all directions.

DISTRIBUTION A. Approved for public release: distribution unlimited.

Toy models for physics

DISTRIBUTION A. Approved for public release: distribution unlimited.

Unexpected link between light & ocean rogue waves

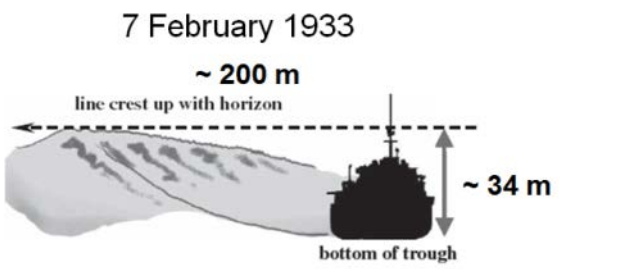

Fig. I.2 Observation of the highest reported wave by the crew members of "Ramapo" (Dennis and Wolff 1996)

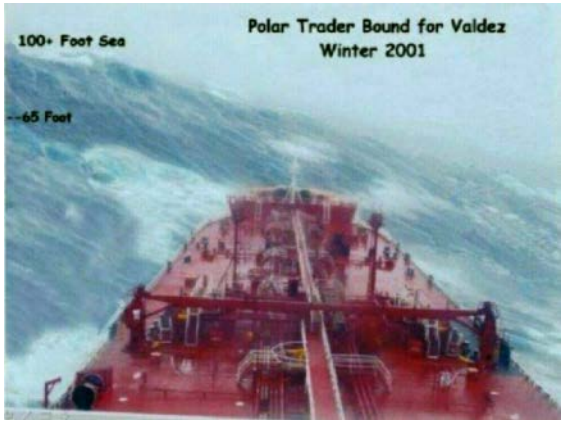

DISTRIBUTION A. Approved for public release: distribution unlimited.

Long tailed statistics in rogue waves & supercontinuum

Ocean Extreme Waves

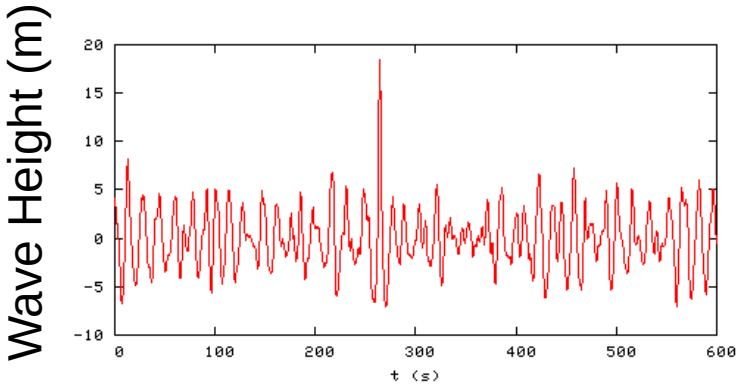

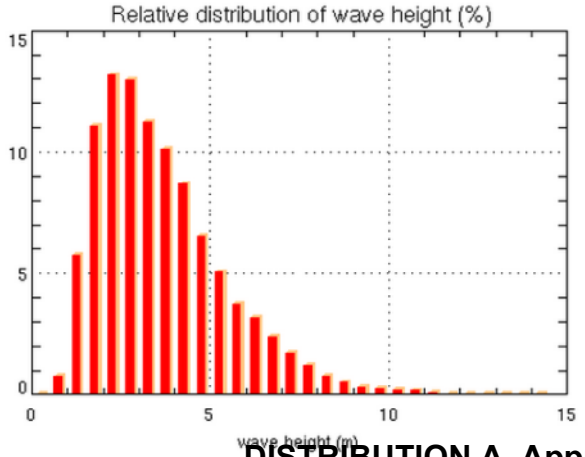

Optical Extreme Waves

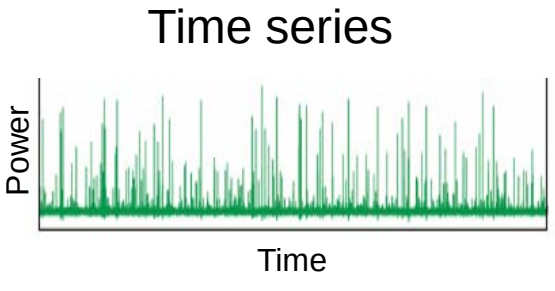

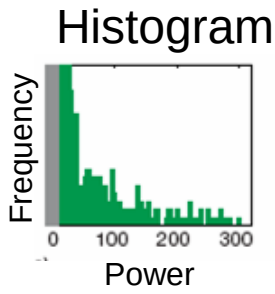

DISTRIBUTION A. Approved for public release: distribution unlimited.

C. Kherif *et al. Rogue Waves in the Ocean*, Springer (2009)

Optical-Ocean Wave Analogy

Deep water ocean wave groups and ultrashort envelopes in optical fibres are both described by the same propagation equation

Nonlinear Schrödinger Equation (NLSE)

Water Waves

$$\frac{\partial A}{\partial t} + i\sigma \frac{1}{8}\frac{\omega_0}{k_0^2}\frac{\partial^2 A}{\partial x^2} + i\beta \frac{1}{2}\omega_0 k_0^2 |A|^2 A = 0$$

***A* is surface elevation of wave group**

$\sigma, \beta \sim 1$ in deep water

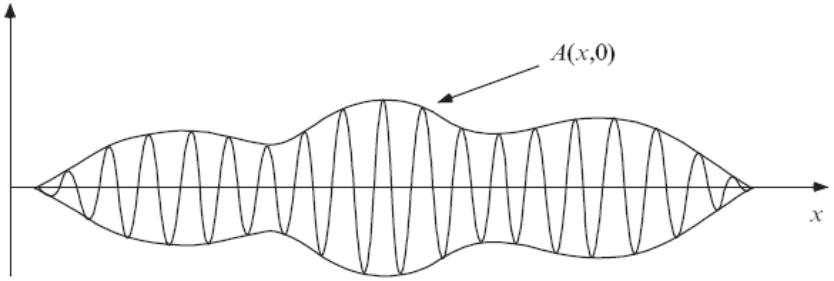

Ultrashort Pulses

$$\frac{\partial A}{\partial z} + i\frac{\beta_2}{2}\frac{\partial^2 A}{\partial T^2} - i\gamma |A|^2 A = 0$$

***A* is amplitude of pulse envelope**

$\beta_2 < 0$ group velocity dispersion

γ nonlinearity

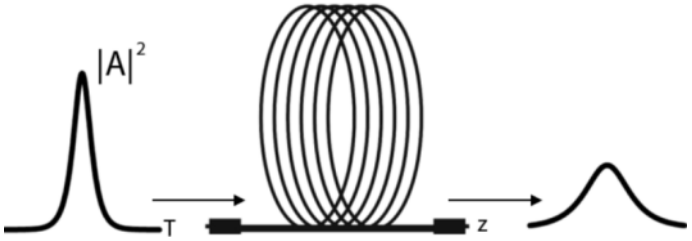

Optical and water waves have same nonlinearity – speed depends on intensity

DSTO-WAVES-A Approved for public release; distributed unlimited

Experiments

We can excite families of solitons on finite background using appropriate input conditions into an optical fibre

$$i\psi_\xi + \frac{1}{2}\psi_{\tau\tau} + |\psi|^2\psi = 0$$

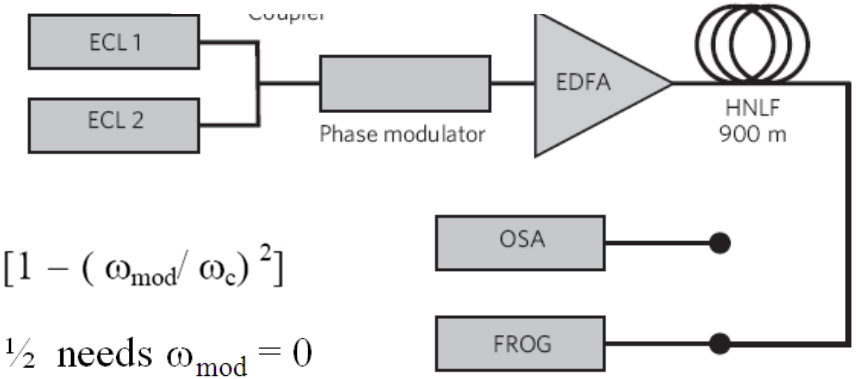

$$2a = [1 - (\omega_{mod}/\omega_c)^2]$$

$$a = \tfrac{1}{2} \text{ needs } \omega_{mod} = 0$$

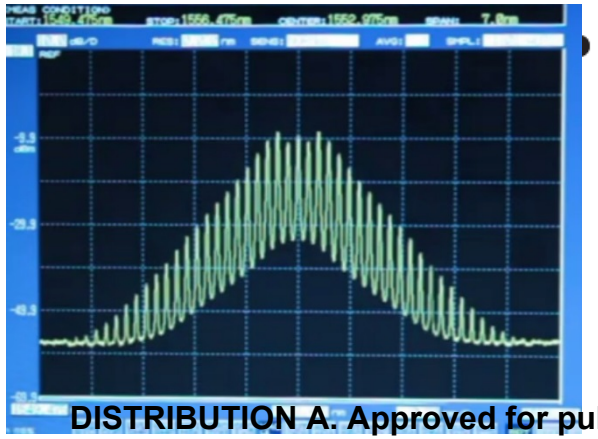

Frequency

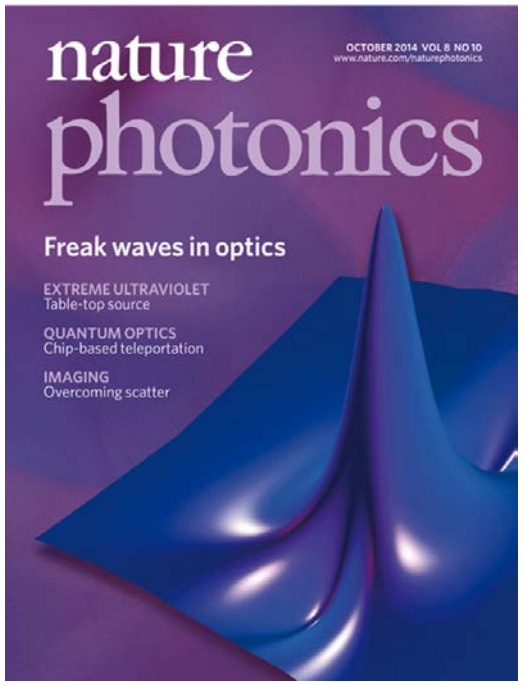

October 2014

DISTRIBUTION A. Approved for public release: distribution unlimited.

Solitons on Finite Background (SFB)

SFBs have been excited in optics using multi-frequency fields

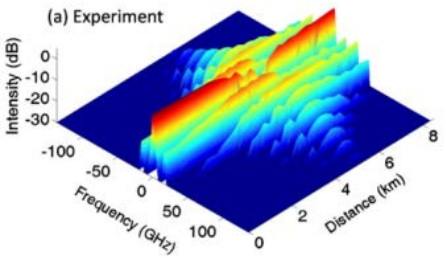

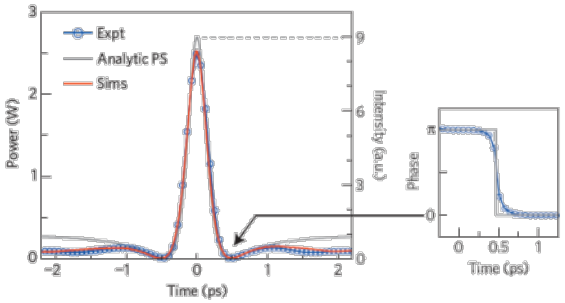

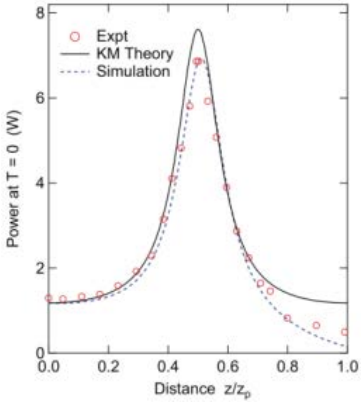

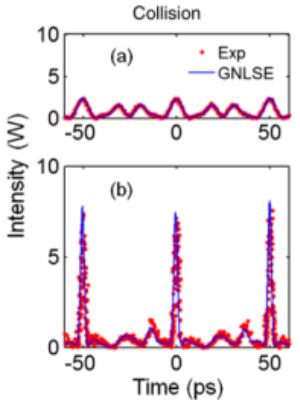

$0 < a < 1/2$

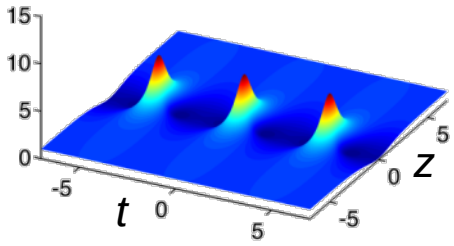

Akhmediev breather (AB)

Hammani *et al*., OL (2011)

$a = 1/2$

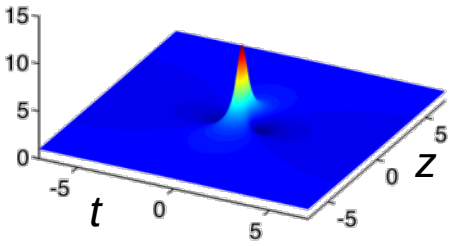

Peregrine soliton (PS)

Kibler *et al*., Nat. Phys. (2010)

$1/2 < a$

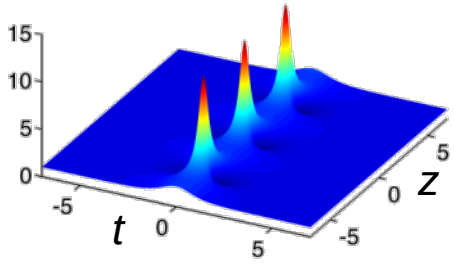

Kuznetsov-Ma soliton (KM)

Kibler *et al*., Sci. Rep. (2012)

(a, a')

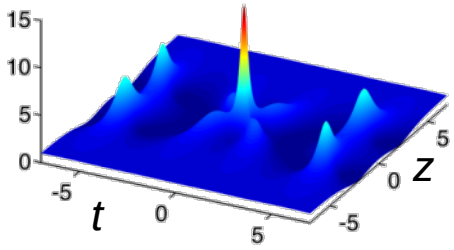

Higher-order AB

Frisquet *et al*., PRX (2013)

DISTRIBUTION A. Approved for public release: distribution unlimited.

Motivating experiments in hydrodynamics

OPEN ACCESS Freely available online

PLOS ONE

Rogue Waves: From Nonlinear Schrödinger Breather Solutions to Sea-Keeping Test

Miguel Onorato[1,2], Davide Proment[3]*, Günther Clauss[4], Marco Klein[4]

1 Dipartimento di Fisica, Università degli Studi di Torino, Torino, Italy, **2** INFN, Sezione di Torino, Torino, Italy, **3** School of Mathematics, University of East Anglia, Norwich, United Kingdom, **4** Ocean Engineering Division, Technical University of Berlin, Berlin, Germany

DISTRIBUTION A. Approved for public release: distribution unlimited.

Light & gravity

nature COMMUNICATIONS

ARTICLE

Received 14 Mar 2014 | Accepted 12 Aug 2014 | Published 17 Sep 2014

DOI: 10.1038/ncomms5969

Nonlinear optics of fibre event horizons

Karen E. Webb[1], Miro Erkintalo[1], Yiqing Xu[1,2], Neil G.R. Broderick[1], John M. Dudley[3], Goëry Genty[4] & Stuart G. Murdoch[1]

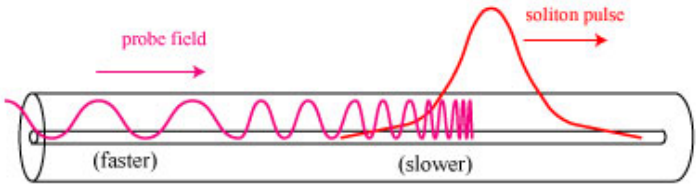

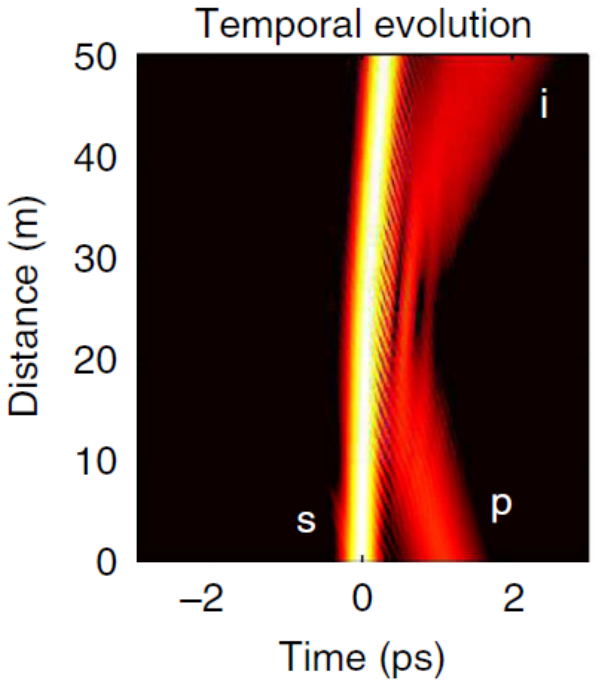

Observation of Gravitational Effects in Nonlocal Nonlinearity

Rivka Bekenstein [1], Ran Schley [1], Maor Mutzafi [1], Carmel Rotschild [1], Ido Dolev [2], Ady Arie [2] and Mordechai Segev [1]

[1]*Physics Department and Solid State Institute, Technion, 32000 Haifa, Israel*
[2]*Department of Physical Electronics, Fleischman Faculty of Engineering, Tel Aviv University 69978, Israel*
* msegev@tx.technion.ac.il

Abstract: We demonstrate optical analogues of gravitational effects such as gravitational lensing, tidal forces and gravitational redshift in the Newton-Schrödinger mainframe, by utilizing long-range interactions between solitons and accelerating beams in nonlocal nonlinear media.

DISTRIBUTION A. Approved for public release: distribution unlimited.

Summary

Ultrashort pulses of light are finding new applications in unexpected ways

Optical fibre supercontinuum

Shaped light for material processing

Toy models of physics

DISTRIBUTION A. Approved for public release: distribution unlimited.